6
参赛学生姓名:Yihao Li
中学:Shenzhen Middle School
省份: Guangdong
国家/地区: China
指导老师姓名: <u>Mingjie Zhang, Nan Hu</u>
指导老师单位: Southern University of
Science and Technology, Shenzhen Middle
School
论文题目: <u>Design a "Molecular Universe" within</u>
Cells: Exploring Liquid-Liquid Phase
Separation and the Design of Biological
Condensates
5,14,

Design a "Molecular Universe" within Cells: Exploring Liquid-Liquid Phase Separation and the Design of Biological Condensates

Yihao Li

1. Abstract

Gravity is the natural force that keeps stars and galaxies moving in an orderly fashion across the vast universe. But what drives the organized distribution and function of countless tiny structures inside a cell? This kind of cross-scale thinking led me to a cutting-edge topic in life science: liquid—liquid phase separation (LLPS), which drives the formation of membraneless organelles inside cells. Protein condensates formed through LLPS play crucial roles in organizing cellular processes. Engineered condensates offer a powerful tool for deliberately programming and modulating cellular activities. Although scientists are beginning to understand how LLPS drives the formation and function of biological condensates, one major challenge remains — how can we rationally design multi-phasic condensates inside living cells?

It all started when I noticed lots of tiny dark droplets while dipping my bread in olive oil and vinegar at breakfast. Watching the tiny dark droplets float, merge, and move like little planets in space made me wonder why they didn't mix completely. That small dish became my window into the mysteries of liquid-liquid phase separation. I began exploring this question in the synthetic biology lab at Shenzhen Middle School, where I observed LLPS phenomenon using everyday materials such as oil, vinegar, lychee rose syrup, and blueberry-flavored Gatorade. I tested how temperature, salt concentration, and pH affected the formation of phase-separated droplets. The results showed that the interface formation time in the oil–vinegar system decreased with increasing salt concentration, while the dissolution time of oil–vinegar and syrup mixture decreased as the temperature increased, and acidification prolonged the rehomogenization time of oil–vinegar and syrup mixture. These findings confirmed the regulatory factors for LLPS regulation.

Next, I developed a synthetic biology approach to engineer multi-phase protein condensates by incorporating specific, orthogonal interaction pairs between scaffold proteins. I systematically characterized two sets of orthogonal condensate systems

composed of special scaffold proteins that naturally form droplets through distinct molecular interaction networks. These scaffold proteins were designed to be orthogonal, meaning they do not interfere with one another's condensate formation. This allowed us to create synthetic condensates that remain separate, offering a flexible and powerful platform for building more complex structures by adding linker between them. Building on this foundation, I introduced well-characterized interaction pairs to act as molecular linkers between orthogonal condensates. By tuning the interaction strength and the abundance of linker pairs fused to the scaffold proteins, I achieved programmable assembly of immiscible condensate phases *in vitro*. Using doxycycline-induced Tet-on expression of a free bridge linker that binds to both condensates, I successfully generated phase-in-phase multi-phasic condensates in heterologous cells.

These designer multi-phasic condensates provide a versatile platform for synthetic biology applications, potentially enabling precise control over reaction compartmentalization and biomolecular organization in engineered systems. This strategy opens new avenues for constructing advanced synthetic organelles and optimizing metabolic pathways in living cells.

Keywords:

Liquid-liquid phase separation (LLPS), Orthogonal scaffold proteins, Specific linker pairs, Multi-phasic condensates.

Table of contents

1. Abstract	2
2. Research Background	6
2.1 From Nebulae to Cellular Droplets: my Cross-Scale Inquiry into Self-Organization) 6
2.2 How Do Cells Make Compartments without Walls: Liquid–L	id / 8
2.3 How Proteins Drive Phase Separation: LCDs/IDRs and Multiva Interactions	lent 10
2.4 The Design of Multi-Phasic Condensates: Challenges and Opportunities	11
3. Biological Questions and Research Ideas	_ 13
4. Materials and Methods	16
4.1 Bacterial strain, Household substances, Constructs and Peptic	les 16
4.2 Protein expression and Purification	16
4.3 Protein Labeling with the Fluorophores	_ 17
4.4 Sedimentation-based Phase Separation assay	_ 17
4.5 Imaging-based Phase Separation assay	_ 17
4.6 Isothermal Titration Calorimetry (ITC) assay	18
4.7 Size Exclusion Chromatography coupled with Multi-angle Light Scattering (SEC-MALS) assay	t 18
4.8 HeLa cell Imaging	18
4.9 Statistical analysis	18
5. Results	19
5.1 Breakfast Droplet-Inspired Thinking: Modelling Liquid-Liquid Pl Separation in Household Substances	nase 19
5.2 Select two "Molecular Planets" for Designing "Molecular Universe": Two Orthogonal Scaffolds Protein for Building Multi-Ph	nasic
Condensates	23

5.3 Select two "Molecular Gravity" for Designing "Molecular Universe": Two Adjustable Linker Pairs for Programming	
Condensates Communication	31
5.4 The Strength of the Gravitational Field Matters: Linker Strengt Controls Scaffold Complex Formation	h 35
5.5 Simulate the Orbital paths of Planets by assembling "Molecular Planet and Gravity": Linker Affinity and Amount Orchestrate Condensate Shapes	ar 38
5.6 Testing the Controllable Operating System of an "Artificial Plan Programmable induction of Phase-in-Phase Architectures in Cells	
6. Summary	48
7. Discussion	49
8. References	52
9. Acknowledgements	54
5	

2. Research Background

2.1 From Nebulae to Cellular Droplets: my Cross-Scale Inquiry into Self-Organization

As a high school student passionate about astrophotography, I have often been captivated by the intricate, ordered structures of nebulae and galaxies emerging from the apparent chaos of the cosmos (Fig. 2.1). This fascination with macroscopic order sparked a cross-scale inquiry when, in biology class, I noticed striking morphological similarities in the microscopic world of the cell: the nucleolus resembling a galactic core, the endoplasmic reticulum, mitochondria resembling star clusters, and the membrane-less organelles reminiscent of a vast nebula (Fig. 2.2). This similarity is not mere coincidence; it suggests a universal physical principle—self-organization. Both cosmic systems, governed by gravity, and biological systems, driven by chemical interactions, are examples of open, far-from-equilibrium systems that spontaneously generate complex, stable patterns through the collective behavior of their individual components.

The theoretical foundation for this phenomenon was laid by Nobel laureate Ilya Prigogine, who described such systems as dissipative structures. These structures maintain their internal order by continuously consuming energy and matter from their surroundings and dissipating entropy—a process he termed "order out of chaos." In cell biology, one key physical mechanism for achieving such self-organization is liquid–liquid phase separation (LLPS)¹.

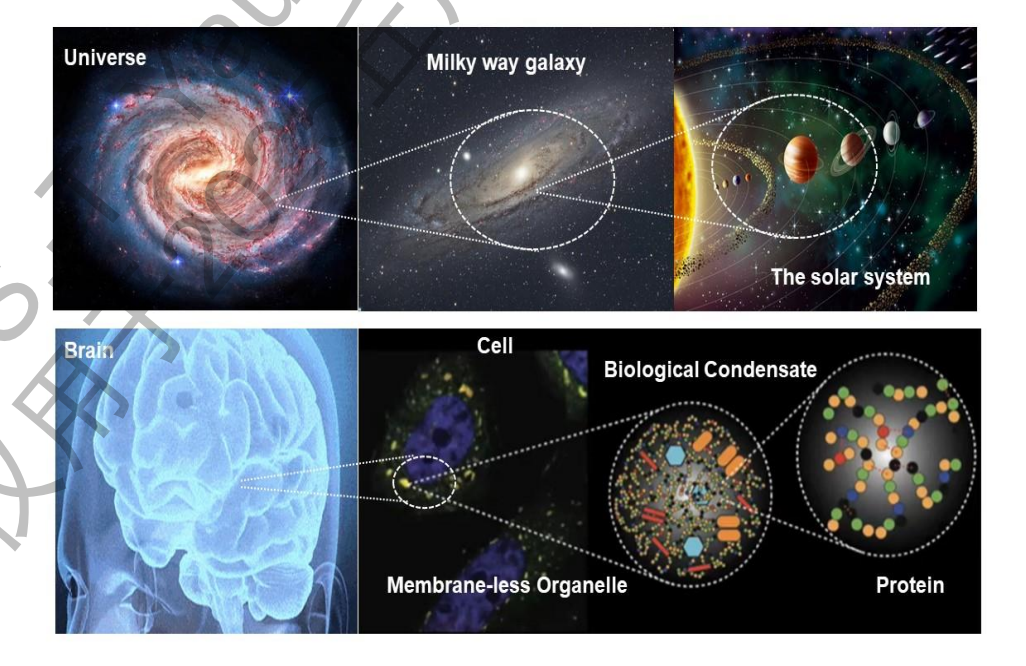


Fig. 2.1 An illustrative diagram comparing the macroscopic view of cosmic nebulae with the microscopic world of cellular structures. The image download from Internet and organize by myself.

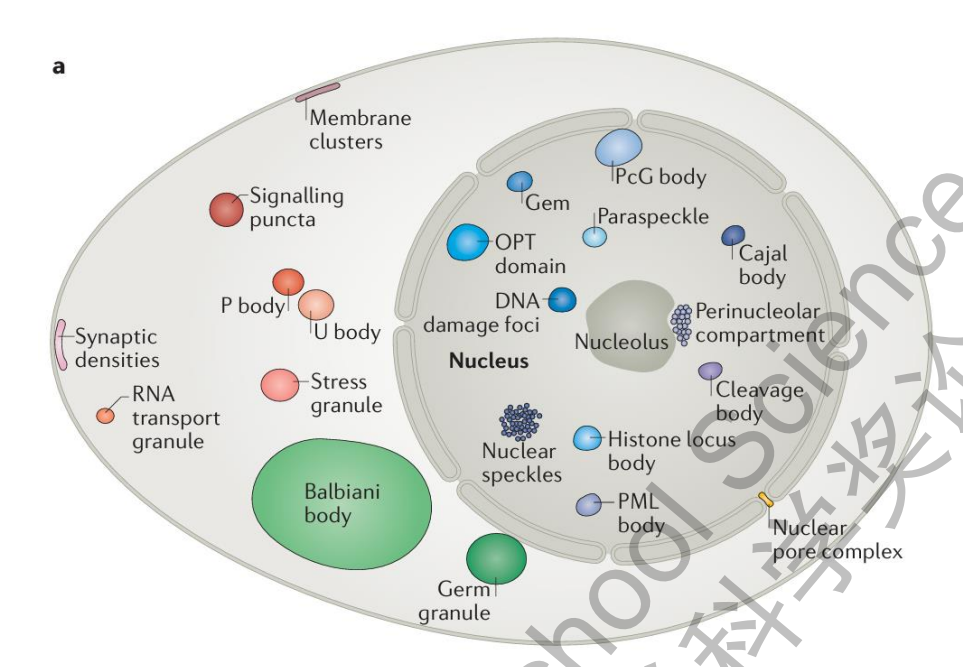


Fig. 2.2 Schematic description of the numerous condensates in the nucleus, cytoplasm and membranes of eukaryotic cells (Salman F. Banani et al; Nat Rev Mol Cell Biol, 2017)

LLPS allows cells to rapidly and reversibly compartmentalize proteins and nucleic acids into distinct, non-membrane-bound organelles, thereby creating specific microenvironments for biochemical reactions to occur in a coordinated fashion². While the principles governing the formation of single-phase condensates are becoming revealed, a significant frontier in synthetic biology remains: the rational design of multiphasic condensates. Natural systems, such as the multi-phase nucleolus, demonstrate a remarkable capacity for creating nested, functionally distinct liquid compartments. However, the "design rules" that govern the formation, stability, and interfacial properties of these complex architectures are poorly understood³. This gap in knowledge presents a major barrier to engineering sophisticated synthetic organelles with multiple, coordinated functions. Therefore, this research addresses a central scientific question: Can we establish a molecular engineering strategy to rationally design and predictably control the architecture of multi-phase protein condensates by programming the interactions at their interface?

2.2 How Do Cells Make Compartments without Walls: Liquid-Liquid Phase Separation

For over a century, a fundamental puzzle perplexed cellular biologists: how could cells create distinct compartments crucial for life processes without the lipid membranes defining organelles like the nucleus⁴? And structures like P granules were clearly visible, performing essential roles in RNA processing, stress response, and development, yet they lacked any physical barrier. Scientists studying P granules in worm embryos witnessed something astonishing: these granules dripped and fused together like liquid droplets⁵ (Fig. 2.3). This wasn't a static structure; it was a dynamic, liquid-like compartment spontaneously forming within the cell.

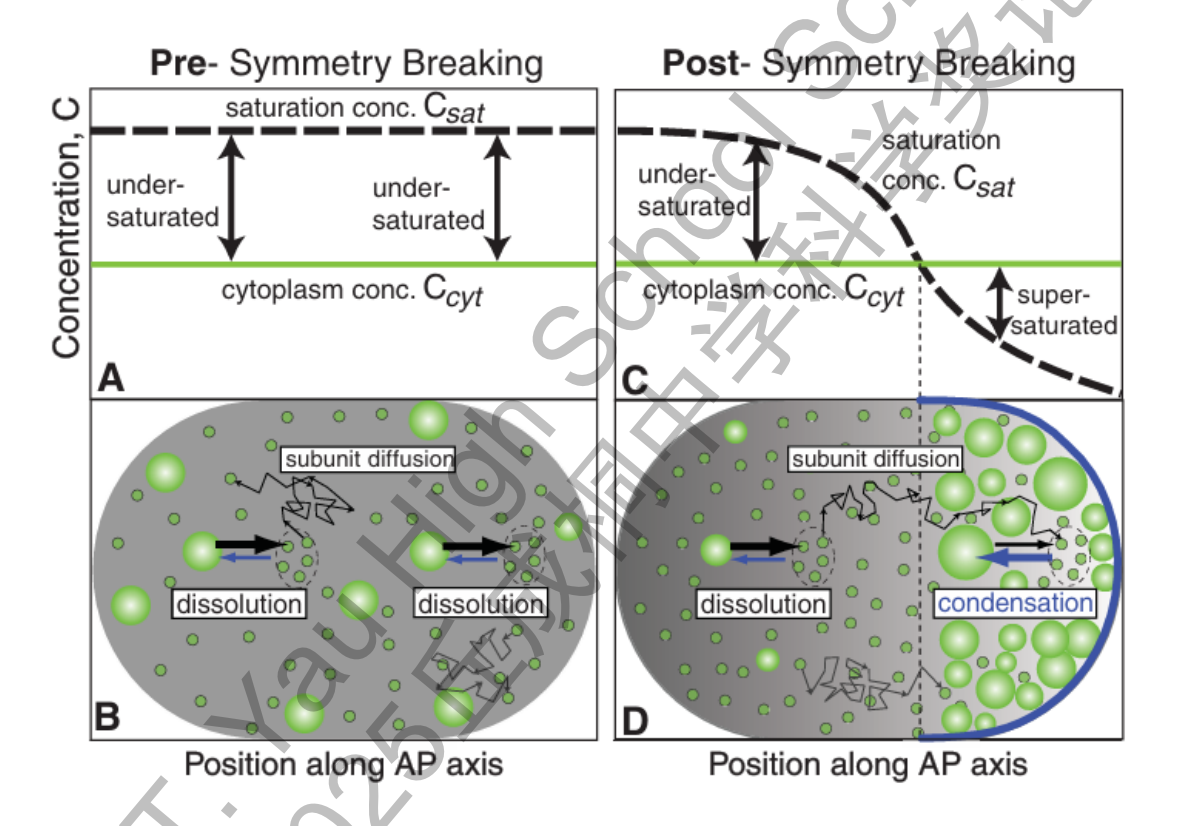


Fig. 2.3 Localized Dissolution and Condensation of P Granules in *C. elegans* germ cells (Clifford P. Brangwynne et al; Science, 2009)

The diagram below illustrates that biomacromolecule solutions, under specific concentration and environmental conditions, undergo liquid-liquid phase separation (LLPS) similar to an oil-water mixture, forming dense phase droplets (concentrated phase) and a dilute phase. The phase diagram, particularly the binodal, serves as the "map" predicting when this separation occurs. The tie lines demonstrate that the

concentrations of the coexisting phases remain fixed in the separated state; altering the total amount only changes the volume ratio between the two phases. The spinodal reveals the kinetic mechanism of phase separation (nucleation and growth *versus* spontaneous decomposition)⁶. Understanding this diagram is key to comprehending the thermodynamic basis of membraneless organelle (biomolecular condensate) formation (Fig. 2.4).

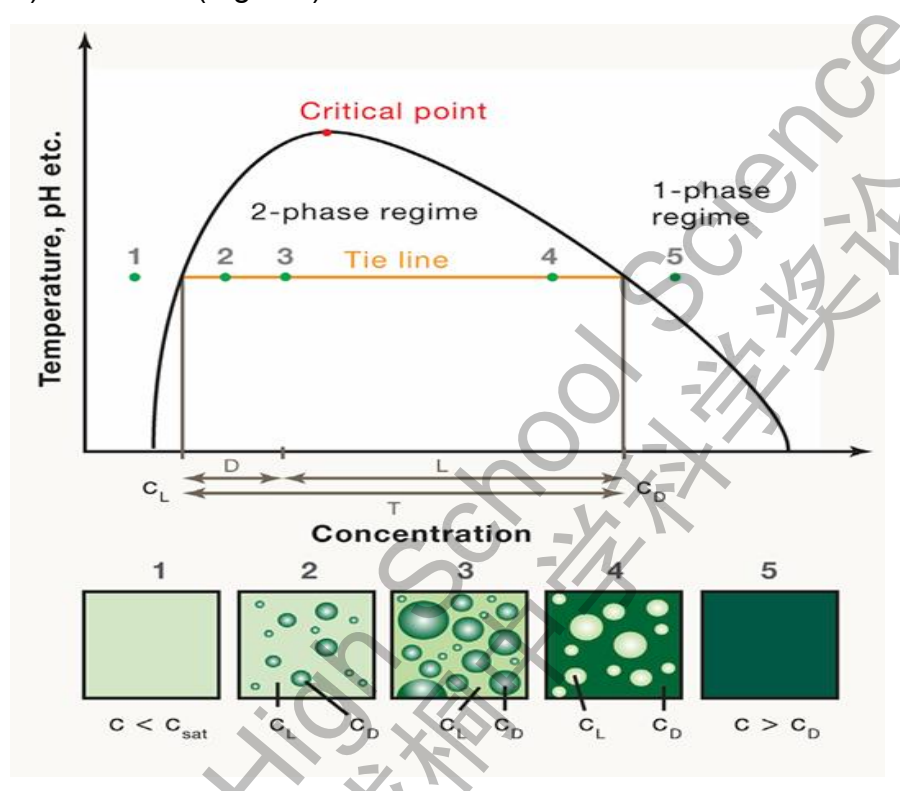


Fig. 2.4 Schematic description of liquid-liquid phase separation diagram (Simon Alberti et al; Cell, 2018)

LLPS elegantly explained how these compartments could form rapidly, reversibly, and membrane-free. The key insight was that specific cellular components, particularly proteins and RNA, could spontaneously demix from the surrounding cellular fluid (cytoplasm or nucleoplasm) to form these distinct liquid phases. This discovery provided a unifying physical principle for a vast array of enigmatic cellular bodies, revealing them as fundamental, evolutionarily conserved organizational units – membraneless organelles. The secret of membraneless organelles wasn't hidden walls; it was biomolecular condensates – dense, liquid-like assemblies forming through a physical process akin to oil separating from vinegar⁷.

2.3 How Proteins Drive Phase Separation: LCDs/IDRs and Multivalent Interactions

Multivalent Interactions via tandem structured domains: Many proteins contain multiple, repeating, folded domains (e.g., RRMs, SH3 domains) or form complexes with multiple binding sites. This "multivalency" allows a single molecule to simultaneously bind multiple partners. When the binding partners are also multivalent, they form large, dynamic networks of interactions⁸. The multivalent connections create the cohesive forces necessary to drive the separation of the mixture into a dense, phase-separated liquid droplet (condensate) and a dilute phase³.

Low-complexity domains and intrinsically disordered regions: Many phase-separating proteins contain regions that lack a stable, folded structure. These LCDs/IDRs often have repetitive sequences and biased amino acid compositions⁹. Specific amino acids drive interactions like cation-π attractions, leading to assembly. Despite disorder, LCDs have a propensity to form transient, labile structures. Hydrogen bonding between backbones also contributes. Evidence suggests these structures are crucial drivers. LCD-driven phase separation is vital for processes like transcription regulation and cell division¹⁰.

Cooperation between Forces: While multivalent domains and LCDs can drive phase separation independently, they often work together in the same protein or complex. The interplay between structured multivalent interactions and LCD-mediated interactions fine-tunes the phase separation behavior and properties of the resulting condensate⁸ (Fig. 2.5).

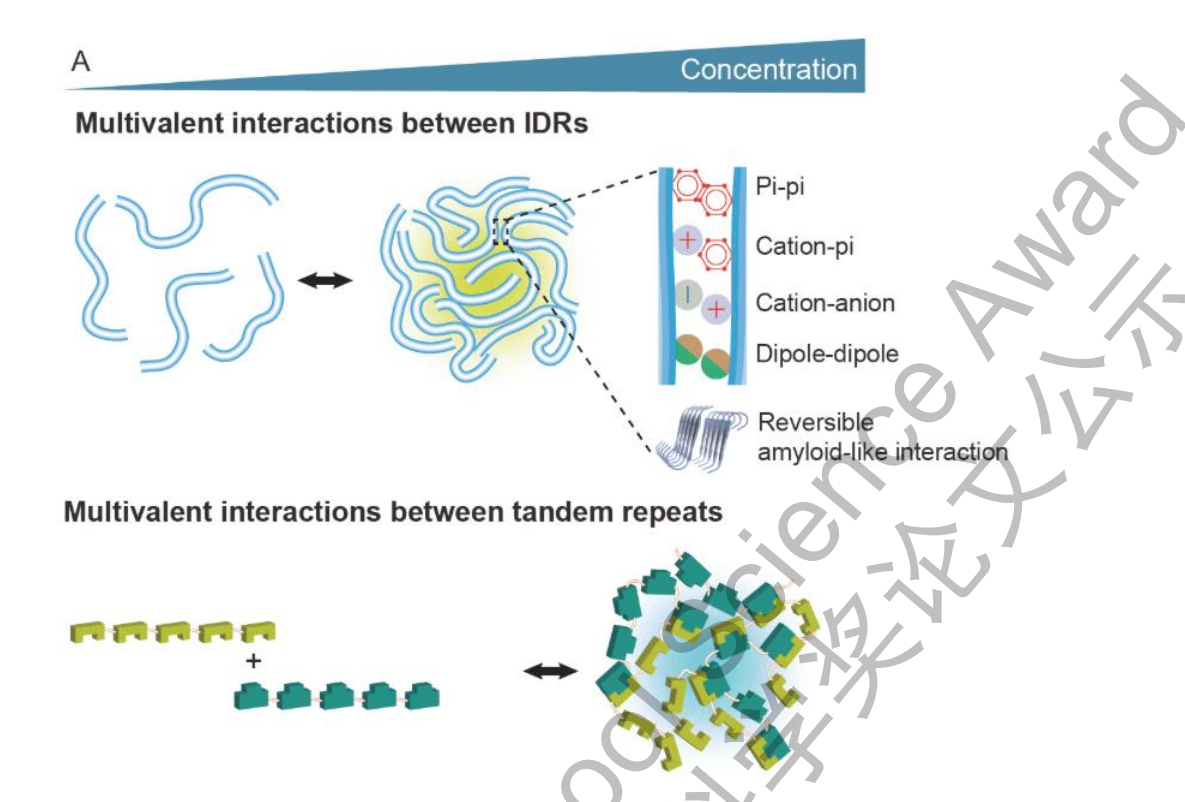


Fig. 2.5 Schematic diagram showing phase separation is driven by multivalent interactions. (Hong Zhang et al; Sci China Life Sci, 2020)

2.4 The Design of Multi-Phase Condensates: Challenges and Opportunities

In synthetic biology, these mechanisms have been repurposed to construct programmable condensates that spatially organize cellular machinery¹¹. For instance, engineered synthetic membrane-less organelles using phase-separating protein scaffolds to sequester endogenous enzymes via high-affinity motifs enable precise control over cellular behaviors such as proliferation and cytoskeletal organization. This enable synthetic biologists to design adaptive organelles, improve bioproduction yields, and complex programming of metabolic pathways¹² (Fig. 2.6).

While scientists have made progress in creating synthetic condensates, designing multi-phase condensates with distinct liquid phases remains a major challenge 13,14. Current systems mainly focus on single-phase condensates for recruiting biomolecules, however these cannot control multiple, orthogonal reactions within designer multi-phase condensate. Multi-phase architectures could enable compartmentalization of incompatible enzymes (for example, opposing metabolic pathways) while maintaining shared metabolite pools. This mimics natural systems, such as nested compartments within the cell nucleus 15.

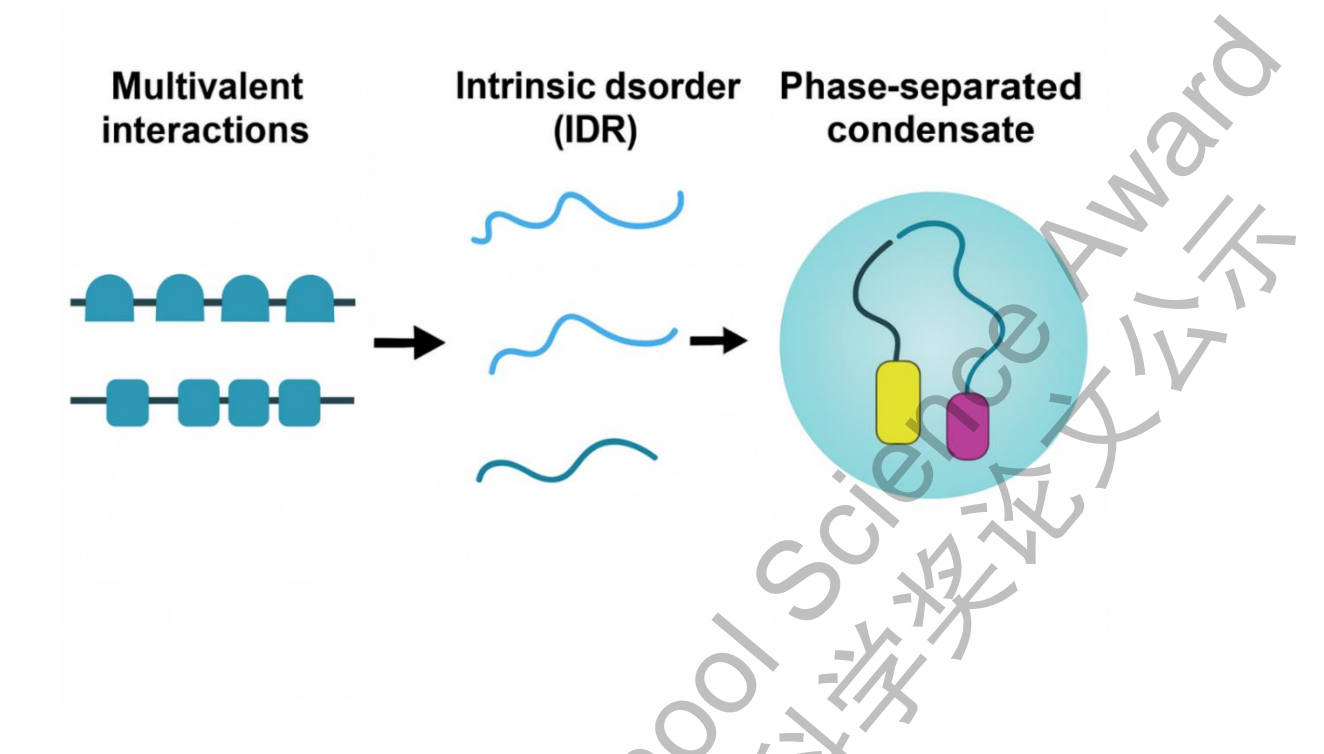


Fig. 2.6 Schematic diagram showing engineering biomolecular condensates.

The rational design of multi-phase protein condensates remains fundamentally challenging due to unresolved mechanistic principles governing their formation and maintenance. Creating stable multi-phase condensates is difficult to me due to three key problems:

- (1) Unclear phase separation rules: I know how single-phase condensate assembly relies on well-characterized multivalent interactions⁸, but I don't fully understand what is the specific molecular features that keep multiple distinct liquid phases distinct (e.g., interfacial tension, differential solubility)¹⁶;
- (2) Missing compatible parts: lacking pairs of engineered protein scaffolds and specific interaction pairs that can form separate droplets *simultaneously* without interfering with each other;
- (3) Instability in cells: Multi-phase systems often become unstable and merge into a single phase. I don't have the tools to predict how the features of scaffold proteins and their specific interaction pairs work together to control multi-phase behavior.

3. Biological Questions and Research Ideas

While the principles governing single-phase condensate formation via multivalent interactions are relatively well understood, the mechanisms that enable the stable coexistence of multiple distinct liquid phases within a single condensate remain elusive. Natural systems, such as the nucleolus, display this multi-phase organization, yet synthetic recreation is hindered by insufficient mechanistic knowledge.

The scientific questions are as follows:

- The lack of well-defined "phase separation rules" for multi-phase systems makes rational design challenging. The default demixing rule can act as a guideline.
- The scarcity of readily available, well-characterized, and truly orthogonal condensate scaffold pairs constrains the construction of multi-component systems. Most synthetic biology studies focus on single-phase condensates that recruit diverse clients, rather than on achieving stable multi-phase coexistence.
- The inability to reliably control interfacial interactions and prevent phase fusion renders engineered multi-phase condensates unstable—particularly in living cells—thereby limiting their potential as synthetic organelles or metabolic engineering platforms.

This study aims to address the critical challenge of rationally designing stable, multi-phase biomolecular condensates. The flowchart below represents the starting point of my research inspiration and the framework of my research concept.

Astrophotography at the observatory	Breakfast at home: Oil a vinegar droplet
A	Cross-Scale Scientific Inspirat
	Literature review with guidance from a mentor

fast at home: Oil and vinegar droplet

Microscopic observation of cellular structures

ale Scientific Inspiration





Preliminary exploration of liquid-liquid phase separation phenomena

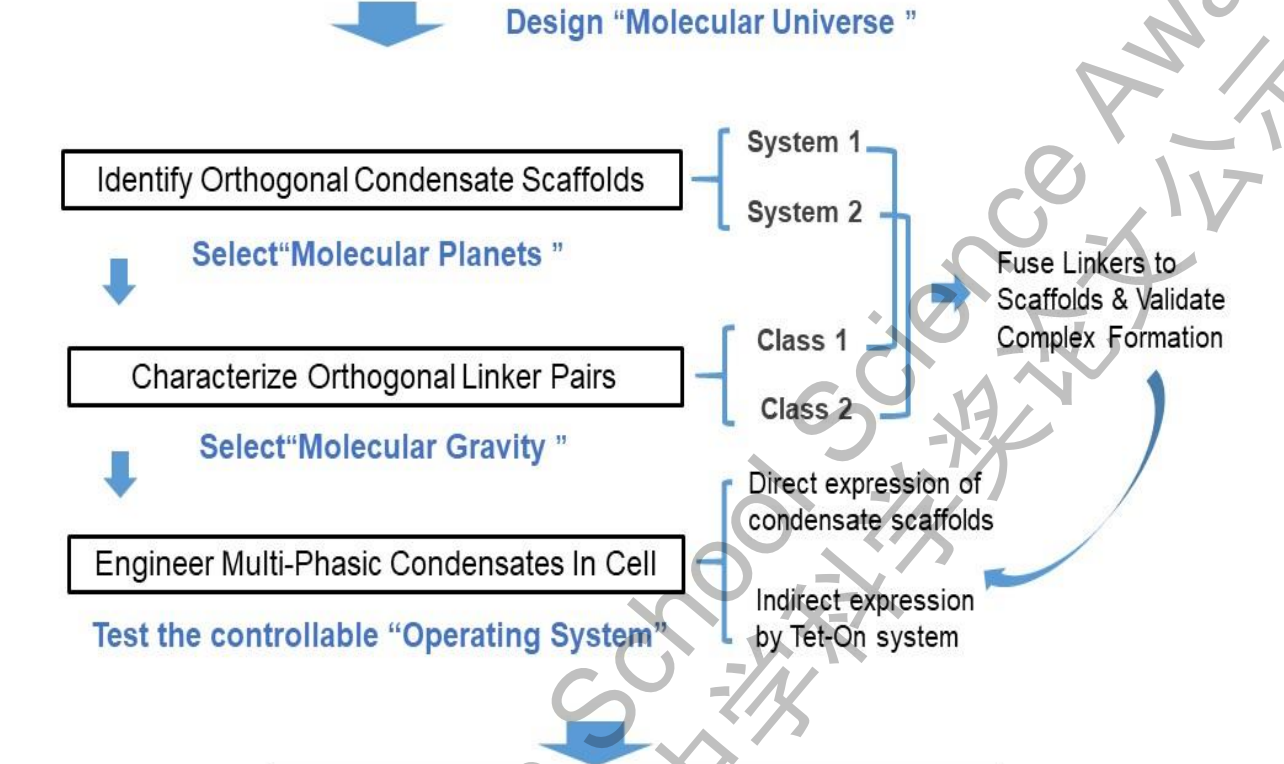


Research question:

How to precisely design stable and multiphasic protein condensate systems

Origins of the Research Idea

Core question: how rational design of stable multi-phasic condensates



Application: Synthesize membrane-less organelles and manipulation of intracellular signaling pathways

Research Path

4. Materials and Methods

Unless specified otherwise, all research materials and facilities used in this project were kindly provided by and all biological phase separation experiments were performed in the Prof. Mingjie Zhang's lab in the School of Life Sciences, Southern University of Science and Technology. All these experiments followed well-established procedures in the Prof. Zhang's laboratory. I describe the key experiments related to this projects briefly below.

4.1 Bacterial strain, Household substances, Constructs and Peptides

E. coli BL21(DE3) cells (Agilent Technologies) were used in this study to produce recombinant proteins. Cells were cultured in LB medium supplemented with necessary antibiotics. Oil-vinegar, syrup-water, settled, gatorade etc. these items obtained from either our shoool synthesis lab or purchase from Meituan and my home. The experiments simulating liquid–liquid phase separation using household materials were primarily conducted in the Synthetic Biology Laboratory at Shenzhen Middle School, with some materials and instruments provided by the Life Science Platform of Southern University of Science and Technology. Plasmids encoding RIM1α_PAS constructed from Rat RIM1a (GenBank: XM_017596673.1) and RBP_(SH3)3 constructed from RIM-BP2 (GenBank: XM_017598284.1) were from previous study¹⁷. The plasmids containing (SUMO)₁₀ and (SIM)₁₀ were obtained from Addgene (#126948, #126946). All constructs were confirmed by DNA sequencing.

4.2 Protein expression and Purification

All proteins were expressed in *E. coli* BL21(DE3) cells in LB medium at 37°C until OD600 reached ~0.6. Protein expression was induced by adding 0.5 mM IPTG at culture temperature (16°C) for overnight. Recombinant proteins were purified with a Ni²+-NTA affinity column (GE Healthcare) followed by size exclusion chromatography (Superdex 75 26/60 for RBP_(SH3)₃ and Superdex 200 for all other proteins). The affinity tag of each protein was cleaved by HRV-3C or TEV protease at 4°C overnight and removed by another step of Superdex 200 26/60 or Superdex S75 size exclusion chromatography with a buffer containing 50 mM Tris pH 8.2, 200 mM NaCl, 1 mM EDTA and 1 mM DTT. A final Mono Q™ anion exchange chromatography step was used to remove remaining nucleic acid contaminations from the full-length MAGl-2. (SUMO)₁₀ and (SIM)₁₀ and PDZ0-GK-(SIM)₁₀ were purified according to the methods described in the previous publication¹8.

4.3 Protein Labeling with the Fluorophores

For amide labeling, the fluorophores including iFluor 405/Cy3/Cy5 NHS ester (AAT Bioquest) and Alexa Flour 488/647 NHS ester (ThermoFisher), were dissolved in DMSO. Purified proteins were exchanged into a buffer containing 20 mM HEPES, pH 8.0, 200 mM NaCl, 1 mM EDTA, and 1 mM DTT by a Hi-Trap desalting column. A fluorophore was added into a protein solution in a 1:1 molar ratio at a typical protein concentration of 100 μ M. The typical protein concentration used in dye labelling was 20 μ M, and the mixture was incubated at room temperate for one hour. The reaction was quenched by 200 mM Tris pH 8.2 and the protein in each reaction mixture was separated from the reaction dye by a desalting column using a column buffer containing 50 mM Tris pH 8.2, 200 mM NaCl, 1 mM EDTA and 1 mM DTT. Fluorescence labelling efficiency of each protein was determined by Nanodrop 2000 (ThermoFisher).

4.4 Sedimentation-based Phase Separation assay

All purified proteins were centrifuged at 16,873 g at 4°C for 10 min to remove possible precipitations before sedimentation-based phase separation assays. Proteins were directly mixed at specified concentrations. The final buffer of the sedimentation assay was 50 mM Tris pH 8.2, 100 mM NaCl, 1 mM EDTA, and 5 mM DTT unless otherwise indicated. For sedimentation-based assays, the total volume of each mixture was 50 μ L. After incubating for 10 min at room temperature, each mixture was centrifuged at 16,873 g at 22°C for 10 min. The supernatant was removed and the pellet was resuspended with 50 μ L of the same assay buffer. Proteins recovered in the supernatant and pellet fractions were analysed by SDS-PAGE with Coomassie Blue R250 staining. The intensity of each protein band on SDS-PAGE gel was quantified by Image J.

4.5 Imaging-based Phase Separation assay

All purified proteins were centrifuged at 16,873 g at 4°C for 10 min to remove precipitations before the microscope-based assays. Proteins were and simultaneously directly mixed at specified concentrations. Each mixture was injected into an inhouse-made chamber composed of a coverslip and a glass slide assembled with one layer of double-sided tape¹⁹. DIC and fluorescent images were captured using a Nikon Ni-U upright fluorescence microscope (with a 60x oil lens) at room temperature or a Zeiss LSM 980 confocal microscope using Zeiss Zen software at 22°C with a 63x oil lens

under the supervision of qualified research staff in the lab. Images were processed with Image J.

4.6 Isothermal Titration Calorimetry (ITC) assay

ITC experiments were performed on a MicroCal VP-ITC calorimeter (Malvern) at 25°C. All proteins or peptides used in this experiment were exchanged to a buffer containing 50 mM Tris pH 8.2, 100 mM NaCl, 1 mM EDTA, and 1 mM DTT. Each titration point was performed by injecting a 10μL aliquot of one protein in the syringe into the cell containing its binding protein. The concentrations of the proteins are indicated in the figures containing each ITC curve. The titration data were fitted with the one-site binding model using Origin 7.0 (Malvern).

4.7 Size Exclusion Chromatography coupled with Multi-angle Light Scattering (SEC-MALS) assay

The SEC-MALS system is composed of a static light scattering detector (miniDAWN, Wyatt), a differential refractive index detector (Optilab, Wyatt), and an AKTA purifier (GE Healthcare). 100 µl sample was injected into a Superdex 200 Increase 10/300 GL column pre-equilibrated with a column buffer containing 50 mM Tris, pH 8.2, 100 mM NaCl, 1 mM EDTA, 2 mM DTT. Data were analyzed by the ASTRA (Wyatt) software.

4.8 HeLa cell Imaging

HeLa cells were cultured in DMEM medium supplemented with 10% fetal bovine serum at 37°C with 5% CO₂. Each confocal imaging dish of cells was co-transfected with 1 µg condensate scaffold containing plasmids with or w/o bridging linker at ~60% cell confluency using ViaFect transfection kit following the instruction of the kit. Transfected cells were live imaged at 16 hrs after transfection using a Zeiss LSM 980 confocal microscope with a 40x oil lens. Cells were incubated in a humidified chamber with 5% CO₂ at 37°C when imaging.

4.9 Statistical analysis

Means \pm SD were used to summarize the data, as specified in figure legends. Statistical analyses use unpaired t test. Significance levels are denoted as $^*P < 0.05$, $^{**}P < 0.01$, $^{***}P < 0.001$, $^{***}P < 0.0001$; ns, not significant. Statistical analyses were performed using GraphPad Prism version 10.1.2.

5. Results

5.1 Breakfast Droplet-Inspired Thinking: Modelling Liquid-Liquid Phase Separation in Household Substances

For me, the ritual of returning home on weekend mornings begins with a simple breakfast: a piece of crisply toasted bread, dipped in a homemade mix of Italian olive oil and dark balsamic vinegar. It was not just a treat for my taste buds; it became the starting point of my scientific exploration. I was always fascinated by watching that shallow dish of oil and vinegar. Countless dark droplets of varying sizes floated on the golden olive oil, like a miniature starry sky. When I dragged a corner of my bread through it, they would rupture, merge, and redistribute themselves, as if they were alive (Fig.5.1a). I was curious: Why don't they mix completely? What force allows these "tiny black planets" to remain independent in their oily universe"? This image was etched deeply into my mind. Then, a few weeks later, in a biology class, the teacher was explaining the internal structures of the cell. An image flashed on the screen that made my heart race—inside the nucleus, there were membrane-less, droplet-like structures that formed through a mechanism called "Liquid-Liquid Phase Separation. In that moment, the scene from my breakfast plate and the image inside the cell overlapped in my mind with a powerful clarity. Wasn't the oil-vinegar mixture in my dish a macroscopic example of liquid-liquid phase separation? The inspiration that spread from my palate to my mind ultimately drove me into the laboratory to explore further. I transformed my macroscopic observations of breakfast droplets into a design blueprint for microscopic "molecular planets." To intuitively illustrate the key physicochemical parameters that govern biomolecular phase separation, I first established several macroscopic model systems using common household substances. This project employs three accessible systems. Oil-vinegar, Syrup, Settled Gatorade. These simple experiments are designed to serve as tangible physical analogs for the complex behaviors observed in our protein systems (Fig.5.1b). By visualizing how ionic strength, temperature, and pH influence phase behavior in these accessible systems, we can build a conceptual foundation for understanding the quantitative data from our molecular-level experiments. Quantified parameters included phase separation, dissolution times and re-equilibration kinetics (Table 1, 2, 3).

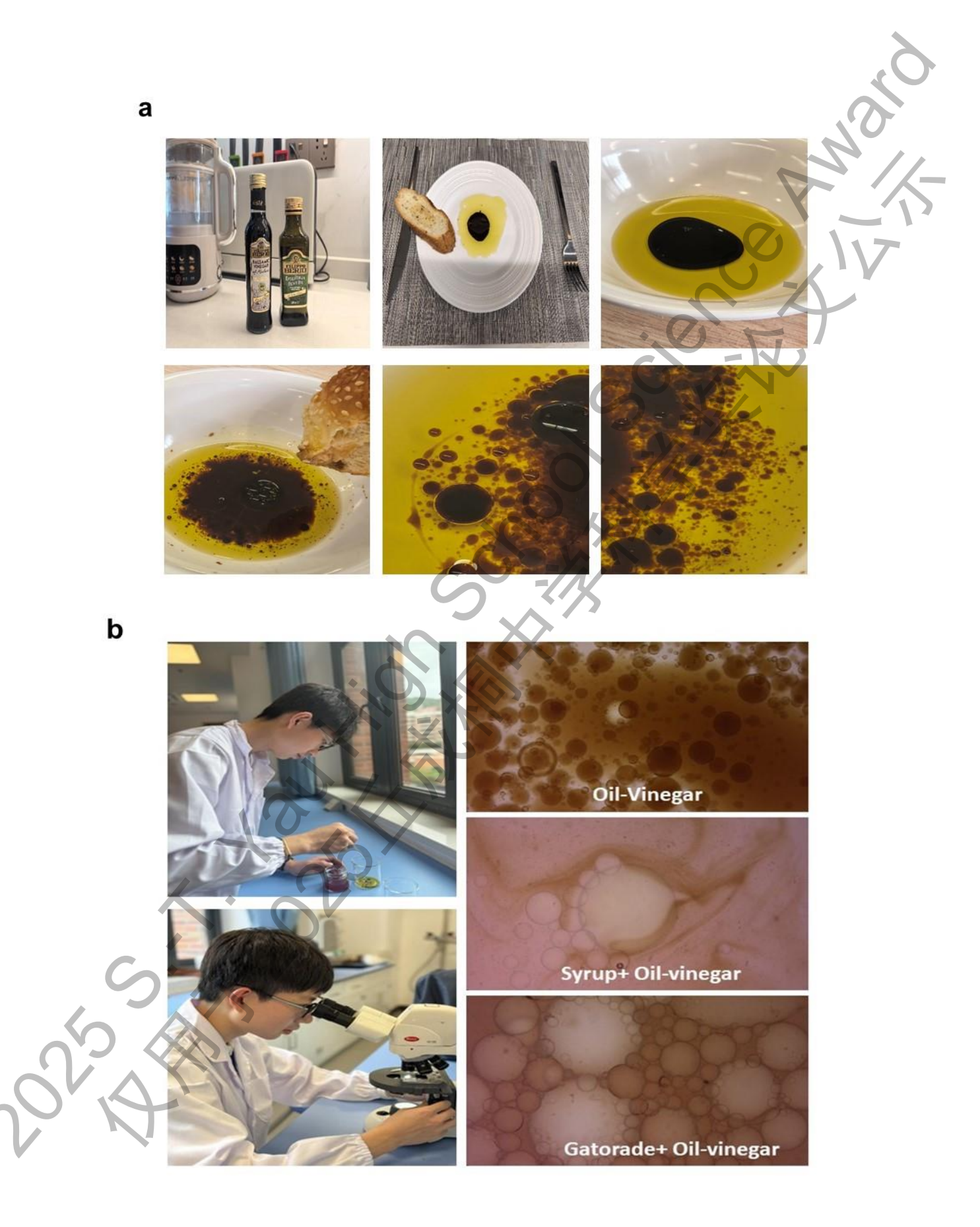


Fig.5.1: Weekend Breakfast at home: Oil and vinegar phase separation. High School Exploration: Studying liquid-liquid phase separation with household items. (a) This photo from a weekend home breakfast, featuring Italian bread dipped in olive oil and vinegar, captures the phase separation of oil and vinegar droplets. (b) These picture show my preliminary exploration of liquid-liquid phase separation using everyday household items in a high school lab. Macroscopic phase separation observation via household items in educational laboratories.

I demonstrate how physicochemical parameters regulate liquid-liquid phase separation (LLPS). Results show as follow:

Table 1: Olive oil-vinegar mixture with varying NaCl concentrations

At room temperature (25 °C), gently pour the mixture, according to a standardized stirring protocol (amplitude/frequency/duration), and let it stand undisturbed to observe the time required for interface formation, assay repeat three times.

NaCI (%)	Interface formation time (min)	Interfacial Phenomena
0	>30	no visible separation
20	12.7 <u>+</u> 2.1	clear oil layer formation
60	6.7 <u>+</u> 1.2	clearly separation

The addition of NaCl introduces ions that strongly compete for hydration, effectively removing water molecules from the surface of the natural emulsifiers in the vinegar. This reduces electrostatic and steric repulsion between oil droplets, promoting their coalescence and accelerating the separation of the dense oil phase from the dilute aqueous phase. This is analogous to the mechanism by which salt concentration modulates protein-protein interactions to drive LLPS.

Table 2: Oil-rose syrup: effect of temperature on Interface formation time

Stir or shake the system to create a transiently mixed or disturbed state. After stopping the stirring, observe and record the time required for the system to form a visually interface, assay repeat three times.

Temp(°C)	interface formation time (min)	Compare to baseline
5	>60	+39% (at least)
25	43.3 <u>+</u> 3.9	0% (baseline)
65	18.7 <u>+</u> 1.7	-57%

Dissolution is a diffusion-limited process, and increasing the temperature provides the requisite kinetic energy for molecules to overcome the activation energy barrier for diffusion and mixing. This same principle governs the molecular mobility within my protein condensates, which I later probe directly with biophysical techniques.

Table 3: Oil- Gatorade: effect of pH on re equilibration time

After stirring or shaking to create a transiently mixed or disturbed state, the system is left undisturbed, and the time required to return to a visually clearly interface state is recorded, assay repeat three times.

Initial pH	Interface formation time (min)	Compare to baseline
3	3.33 <u>+</u> 1.1	-70%
7	10.3 <u>+</u> 2.5	0% (baseline)
12	>60	+500% (at least)

This experiment provides a direct physical analogy to protein liquid—liquid phase separation (LLPS). Proteins, like colloids, possess ionizable surface groups whose net charge depends on the environmental pH. Near the isoelectric point, the net charge of a protein is minimized, leading to reduced electrostatic repulsion and a higher propensity to aggregate or undergo phase separation. Conversely, at pH values far from the isoelectric point, proteins acquire higher net charges that increase repulsive interactions, thereby stabilizing them against LLPS. The oil—vinegar—Gatorade system demonstrates that lowering the pH accelerates aggregation and phase separation by reducing surface charge, whereas raising the pH stabilizes the suspension by enhancing electrostatic repulsion. These findings are consistent with fundamental colloid science and provide an intuitive physical model for understanding how pH modulates protein LLPS in cells.

5.2 Select two "Molecular Planets" for Designing "Molecular Universe": Two Orthogonal Scaffolds Protein for Building Multi-Phase Condensates

When I look at how galaxies are scattered across the universe, it kind of reminds me of how those membrane-less organelles float around inside a cell. In our solar system, there are eight planets, and Earth's closest neighbors—Venus and Mars couldn't be more different. One's a burning world, the other's a frozen desert. That contrast made me curious: what if I could design two membrane-less organelles inside a cell that are completely opposite, just like Venus and Mars? I brought up this idea with my lab mentor and the rest of the team to see what they thought. Recent work in my mentor: Prof. Zhang's lab, I know that they established the complexity and dynamic behavior of percolated molecular networks within condensates are determined by both the binding strengths (affinities) and interaction valencies of their constituent molecules²⁰. In Professor Zhang's lab, on the protein condensate design platform, I selected two types of biomolecular condensates. This two types of condensates with different network properties that are totally orthogonal to each other for the construction of multi-phase condensates. The scaffold proteins of the two condensates are $RIM1\alpha_PAS-RBP_(SH3)_3$ and $(SUMO)_{10}-(SIM)_{10}$, respectively (Fig. 5.2). RIM1α_PAS and RBP_(SH3)₃ are fragments from the presynaptic active zone scaffold proteins RIM and RIM-BP (RBP) (Fig. 5.2a), which form dynamic and condensed assemblies via specific multivalent PRM (proline-rich motif)-SH3 (Src homology 3) domain interaction¹⁷. The other one is a synthetic multivalent condensate system composed of (SUMO)10 (ten tandem repeats of SUMO domain) and (SIM)10 (ten tandem repeats of the SUMO interaction motif) (Fig. 5.2b), which contains highly percolated molecular interaction network between multiple SUMO and SIM¹⁸.

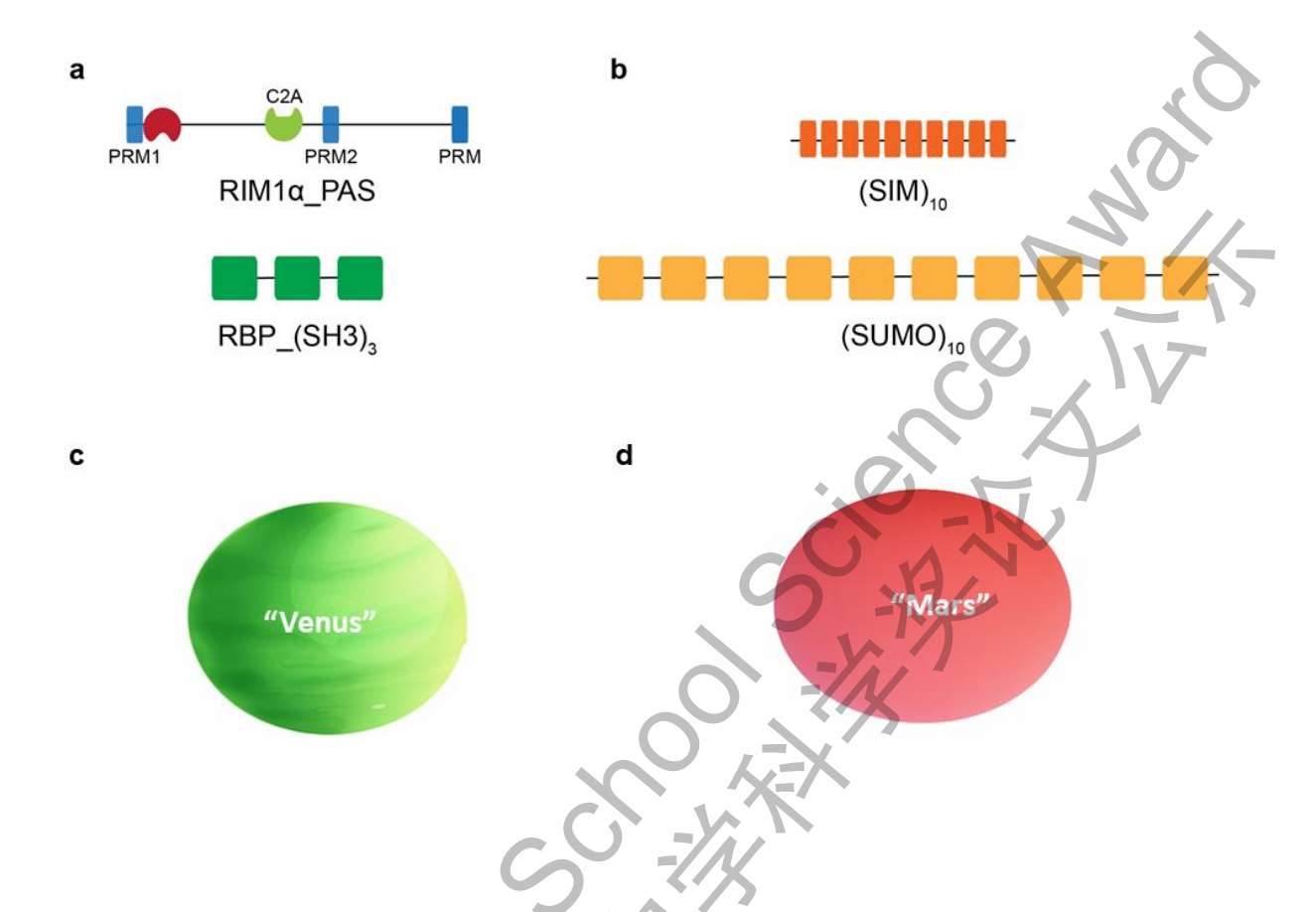


Fig. 5.2: Domain organization of the condensate scaffold proteins and schematic picture of molecular universe.

(a-b) Schematic diagrams of the domain organizations of (SUMO)₁₀ and (SIM)₁₀. (Below) Schematic diagrams of the domain organizations of RIM1 α _PAS and RBP_(SH3)₃. The molecular interaction network exists between SH3 domain and PRM. (c-d) In the schematic diagram, the molecular planet is shown, where Venus represents 'RIM-RBP' condensate and Mars represents 'SUMO-SIM' condensate.

Just like how I'm fascinated by Venus and Mars, I'm really curious to find out what makes these two "molecular planets" so different from each other. I first characterized the biophysical properties of the (SUMO)₁₀–(SIM)₁₀ condensate. Scaffold proteins were purified following established protocols (Fig. 5a)²¹, and their molecular weights were determined using size-exclusion chromatography coupled with multiangle light scattering (SEC-MALS). The measured molecular weights of (SUMO)₁₀ and (SIM)₁₀ were 99.0 kDa and 29.5 kDa (Fig. 5.3b,c), respectively, consistent with their expected sizes and indicating that both proteins exist as soluble monomers in solution. Purified

(SUMO)₁₀ and (SIM)₁₀ were subsequently mixed at varying concentrations, and phase separation was assessed using a sedimentation-based spin down assay.

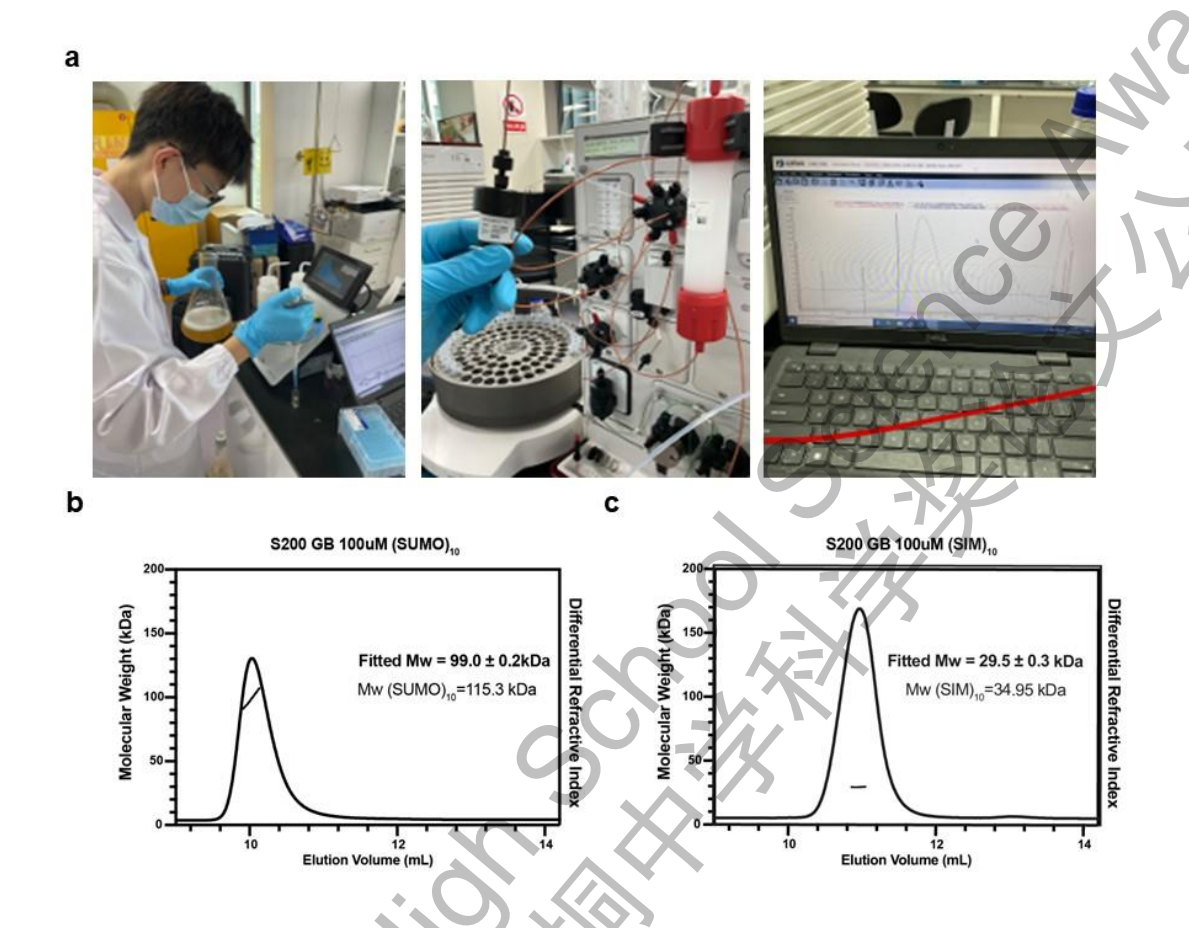


Fig. 5.3: Molecular weight and oligomerization state of (SUMO)₁₀ and (SIM)₁₀.

- (a) Recording the experimental process of protein purification and concentration determination.
- (b) SEC-MALS (size-exclusion chromatography–multiangle light scattering) assay result showing that the fitted molecular weight of (SUMO) $_{10}$ is 99.0 kDa. 100 μ M (SUMO) $_{10}$ was loaded on to the Superdex 200 Increase column balanced with GB (Tris buffered saline containing 50 mM Tris, 100 mM NaCl, 1 mM EDTA, and 1 mM DTT).
- (c) SEC-MALS assay result showing that the fitted molecular weight of (SIM) $_{10}$ is 29.5 kDa. 100 μ M (SIM) $_{10}$ was loaded on to the Superdex 200 Increase column balanced with GB.

Briefly, the two scaffold proteins were combined in general buffer (50 mM Tris, 100 mM NaCl, 1 mM EDTA, 1 mM DTT; abbreviated as GB buffer), and following condensate formation, samples were centrifuged at 15,000 rpm for 10 min at room temperature. Supernatant fractions were carefully collected and mixed with SDS-PAGE loading buffer to generate the supernatant samples (S). Pelleted condensates were resuspended in an equal volume of loading buffer, with additional protein buffer added when necessary to maintain consistent sample volumes between supernatant and pellet fractions (Fig. 5.4). Protein band intensities from SDS-PAGE (Fig. 5a) were quantified, and the proportion of protein in the pellet relative to total input was calculated as the pellet percentage (Fig. 5.5b). Both (SUMO)10 and (SIM)10 exhibited pellet percentages exceeding 60% under all conditions tested, demonstrating robust phase separation (Fig. 5.5c).

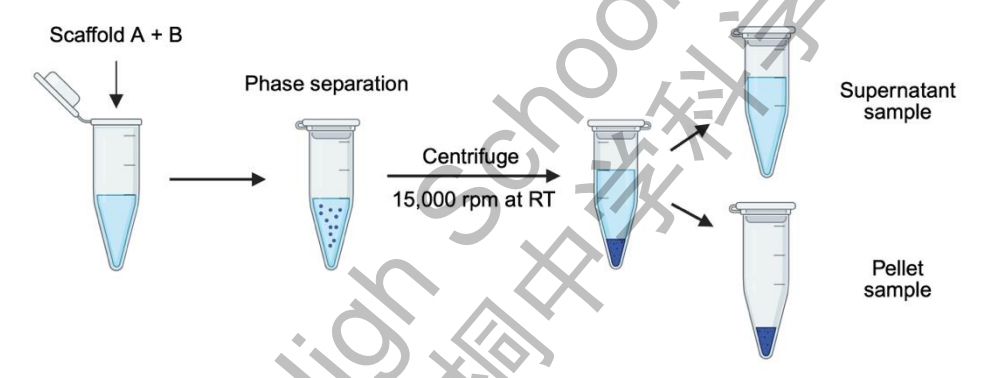


Fig. 5.4: Schematic diagram shows the process of the Spin Down assay.

Schematic diagram showing the process of the Spin Down assay. Briefly, the scaffold proteins are mixed in the proper buffer and phase separate into condensates. Then the reaction tubes are centrifuged at room temperature, 15000 rpm for 10 minutes. The supernatant is transferred to a new tube and add the SDS-PAGE loading buffer into supernatant sample (S). The condensates in the pellet is resuspended with SDS-PAGE loading buffer, and the protein buffer is add to ensure the equal volume between supernatant and pellet samples.

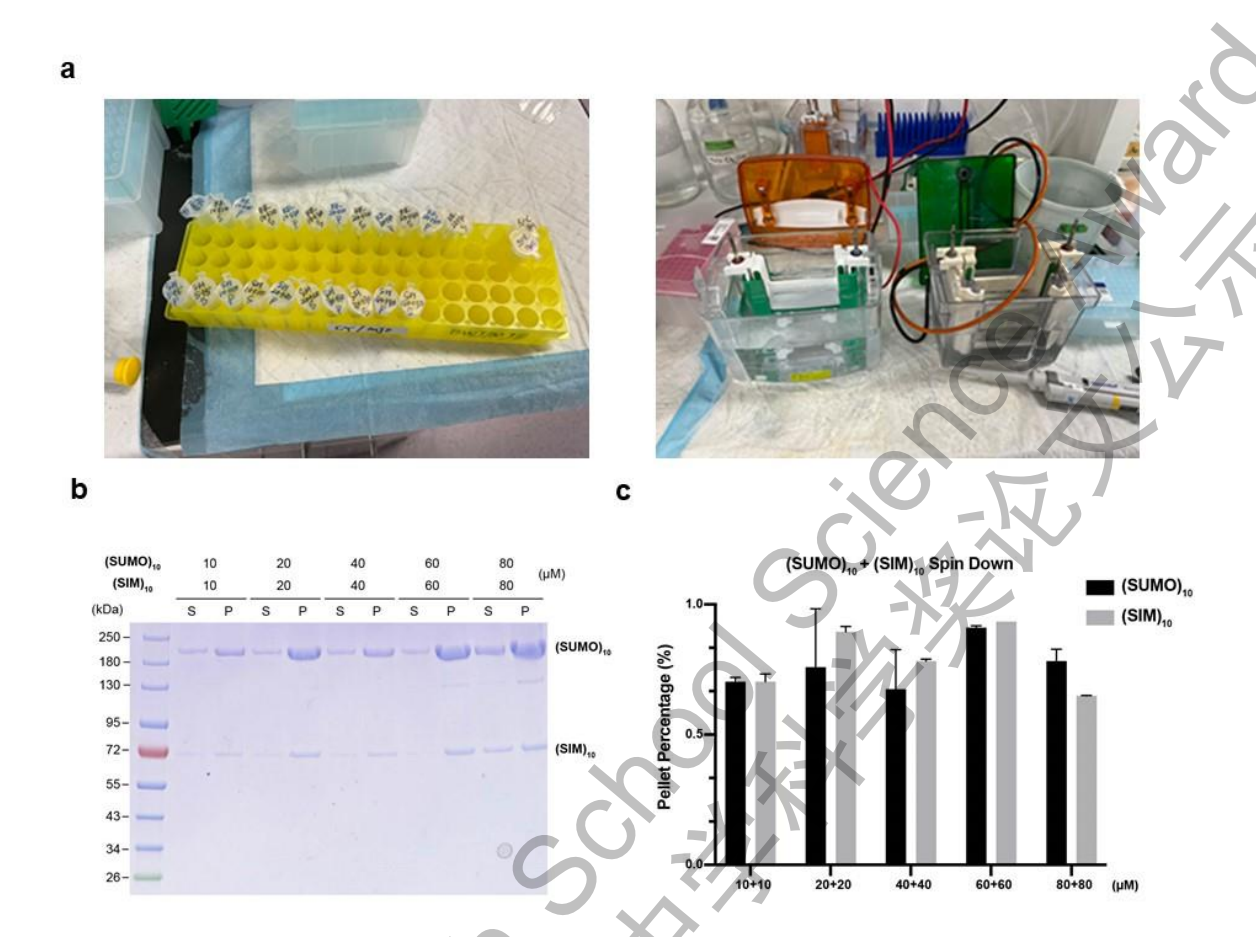


Fig. 5.5: Mixed (SUMO)₁₀ and (SIM)₁₀ phase separate into condensates.

- (a) Performing the SDS-PAGE for the samples from the Spin Down assay.
- (b) SDS-PAGE with Coomassie blue staining showing the Spin Down assay result of mixing different concentration of (SUMO)₁₀ and (SIM)₁₀. The proteins recovered in the supernatant sample were denoted "S" and pellet sample denoted "P".
- (c) The quantification of the pellet percentage in the Spin Down assay shown in panel a, the fractions of proteins recovered in the pellet sample were quantified from three independent repeats of the experiment. Data are presented as mean \pm SD.
- To further probe the molecular interaction network within the condensates, I performed fluorescence recovery after photobleaching (FRAP) experiments to assess molecular mobility. A defined region at the center of individual condensates was photobleached using high-intensity laser illumination, and fluorescence recovery was monitored over time. Recovery within (SUMO)10–(SIM)10 condensates was slow, reaching approximately 25% after 400 s (Fig. 5.6, Fig. 5.10a,c), indicating limited molecule exchange. These observations suggest that (SUMO)10–(SIM)10 condensates

form stable, highly interconnected networks driven by strong multivalent SUMO-SIM interactions.

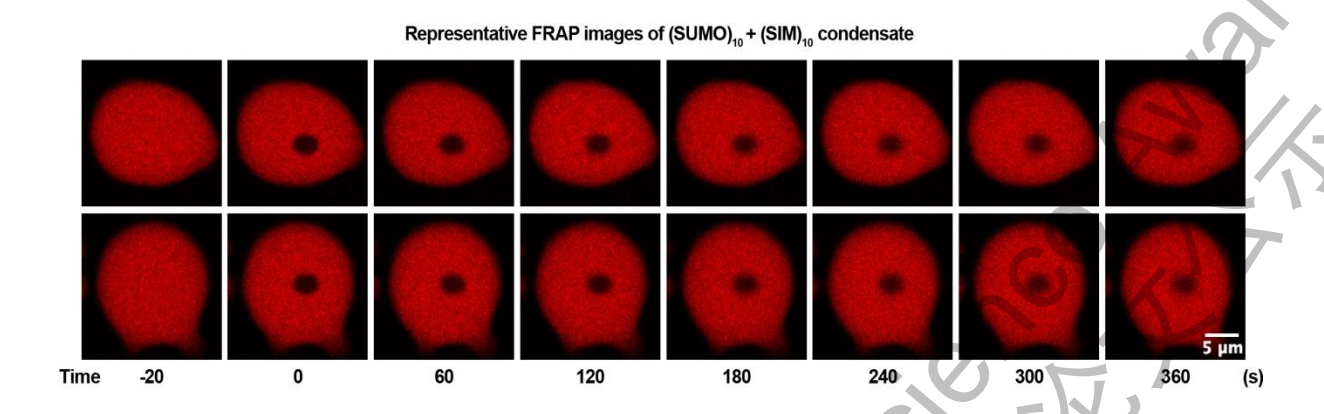


Fig.5.6: The (SUMO)₁₀–(SIM)₁₀ condensate forms stable molecular interaction network. FRAP experiments showing that fluorescence signals from Cy3 labeled (SUMO)₁₀ in the condensed phase recovered very slowly after photo-bleaching. The concentrations of both (SUMO)₁₀ and (SIM)₁₀ were 10 μ M.

To quantitatively characterize the RIM1 α _PAS-RBP_(SH3) $_3$ condensate system, I purified both scaffold proteins and assessed their oligomeric states using SEC-MALS. The experimentally determined molecular weights of RIM1 α _PAS (64.4 kDa, Fig. 5.7a) and RBP_(SH3) $_3$ (32.0 kDa, Fig. 5.7b) were consistent with their theoretical values, confirming that both proteins exist as soluble, stable monomers in solution.

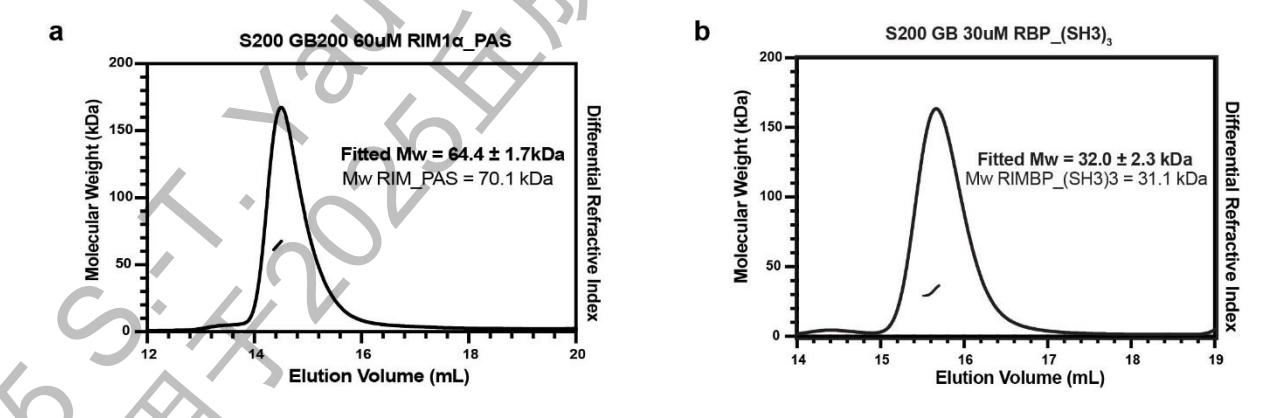


Fig. 5.7: Molecular weight and oligomerization state of RIM1α_PAS and RBP_(SH3)₃.

(a) SEC-MALS assay result showing that the fitted molecular weight of RIM1α_PAS is 64.4 kDa. 60 μM RIM1α_PAS was loaded on to the Superdex 200 Increase column balanced with GB.

(b) SEC-MALS assay result showing that the fitted molecular weight of RBP_(SH3)₃ is 32.0 kDa. 30 μM RBP_(SH3)₃ was loaded on to the Superdex 200 Increase column balanced with GB.

Phase separation was subsequently examined by mixing the two scaffolds at varying molar ratios, which consistently resulted in the formation of condensates via LLPS (Fig. 5.8a). Quantitative sedimentation-based spin-down assays revealed a concentration-dependent increase in the pellet fraction for both proteins, with phase separation efficiency enhanced by increasing either the RIM1 α _PAS:RBP_(SH3)3 molar ratio or the total protein concentration (Fig. 5.8b). Notably, equimolar mixtures at higher concentrations (20 μ M + 20 μ M) exhibited significantly greater partitioning into the condensed phase compared to lower-concentration mixtures (10 μ M + 10 μ M), demonstrating that LLPS is strongly favored under elevated scaffold concentration. FRAP experiments further revealed rapid molecular exchange within the condensates, with approximately 90% fluorescence recovery observed within 400 seconds. These findings indicate that RIM1 α _PAS-RBP_(SH3)3 condensates retain liquid-like properties despite being organized through multivalent interaction networks.

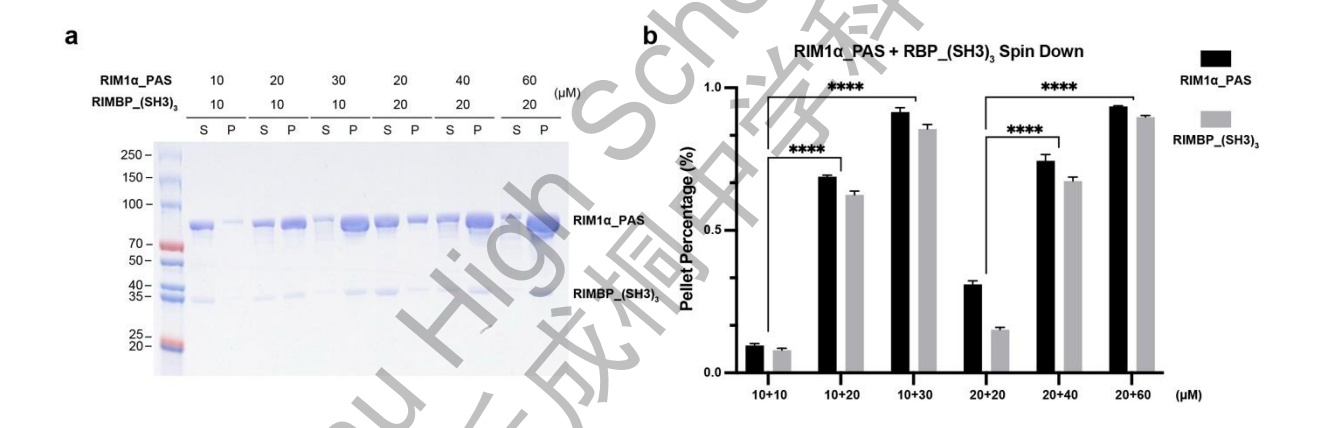


Fig. 5.8: The molar ratio between RIM1 α _PAS and RBP_(SH3) $_3$ determines phase separation strength.

- (a) SDS-PAGE with Coomassie blue staining showing the Spin Down assay result of mixing different ratio of RIM1 α PAS and RBP (SH3)₃.
- (b) The quantification of the pellet percentage in the Spin Down assay shown in panel a, the fractions of proteins recovered in the pellet sample were quantified from three independent repeats of the experiment. Data are presented as mean \pm SD, ****P < 0.0001 for both RIM1 α _PAS and RBP_(SH3)3.

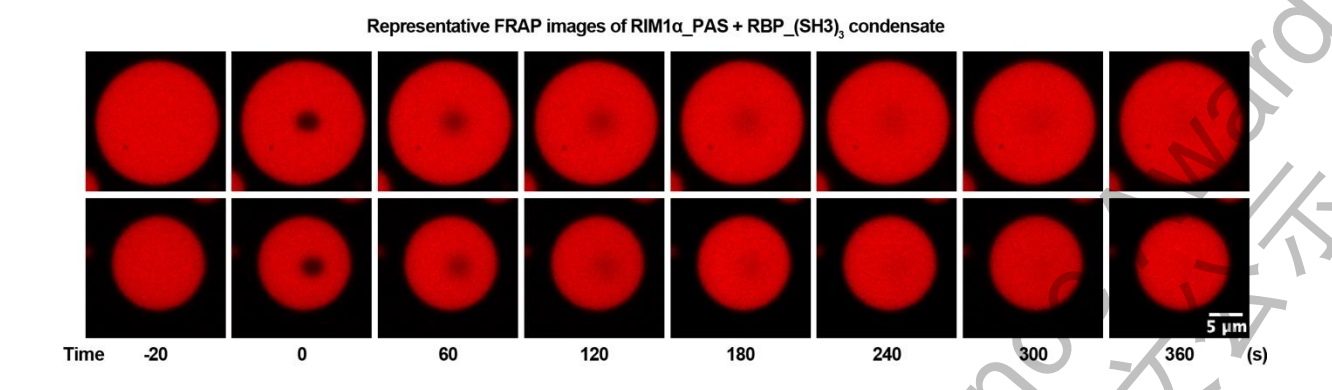


Fig. 5.9: The RIM1α_PAS-RBP_(SH3)₃ condensate is dynamic.

FRAP experiments showing that fluorescence signals from Cy3 labeled RIM1 α _PAS in the condensed phase could fast recover after photo-bleaching. The concentrations of RIM1 α _PAS and RBP (SH3) $_3$ Were 30 μ M and 10 μ M, respectively.

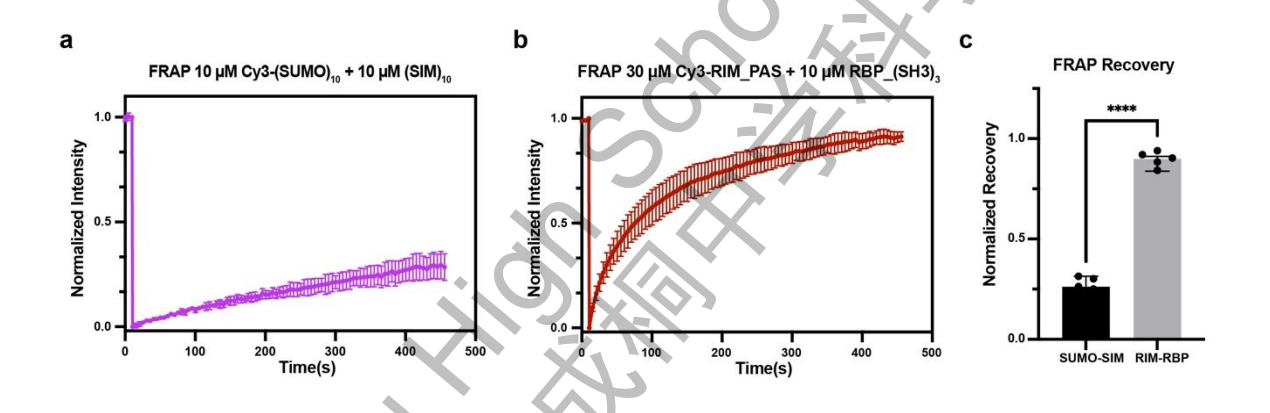


Fig. 5.10: The quantification of FRAP results.

- (a) The curve showing the fluorescence recovery of $(SUMO)_{10} + (SIM)_{10}$ condensate by plotting normalized intensity of the bleached region against time. The averaged signals from 5 droplets with a diameter of 20 mm. Data are presented as mean \pm SD.
- (b) The curve showing the fluorescence recovery of RIM1 α _PAS + RBP_(SH3) $_3$ condensate by plotting normalized intensity of the bleached region against time. The averaged signals from 5 droplets with a diameter of 20 mm. Data are presented as mean \pm SD.
- (c) The normalized fluorescence recovery after photobleaching of 2 kinds of condensates was quantified from 5 independent droplets. Data are presented as mean ± SD.

Molecular Planet	Orthogonal Systems	Core component	FRAP Recovery	Dynamic Property
Venus (High temp, pressure)	RIM-RBP	RIM1α_PAS, RBP_(SH3) ₃	~90%	highly dynamic (liquid-like)
Mars (cold and dry)	SUMO-SIM	(SUMO) ₁₀ , (SIM) ₁₀	~30%	low-dynamic (gel-like)

Table 4: Summary of biophysical properties of the orthogonal condensate systems.

5.3 Select two "Molecular Gravity" for Designing "Molecular Universe": Two Adjustable Linker Pairs for Programming Condensates Communication

Every planet in the solar system orbits the Sun along its designated path. This selforganization is fundamentally driven by a universal force: gravity. In cells, there are myriads of proteins. So, how do they self-assemble into stable, functional, membraneless organelles? And what is the driving force behind their self-organization? It's clear that small molecules interact through molecular forces, but in the case of liquid-liquid phase separation that drives the formation of membrane-less organelles, the driving force comes from multivalent interactions. I think of this as a kind of "molecular gravity" within the cellular solar system. So how could I design different gravitational fields? That's when I thought of using molecular "ropes" with different properties to connect distinct protein condensates, and by tuning the tightness of these molecular ropes, I could control how strongly the condensates bind to each other. After I came up with this idea, Dr. Chen in the lab immediately shared some related papers with me, and that's how I learned that molecular "ropes" or "molecular gravity" actually exist and could help make my idea possible. To reprogram the interfacial contact between orthogonal protein condensates, so I characterized two distinct classes of binding pairs that are strictly orthogonal both to the condensate scaffolds and to one another: (1) heterodimeric coiled-coil peptides (e.g., P3-P4)²², and (2) the Colicin E9 DNase (CL9)–lmmunity2 (IM2) complex²³. Isothermal titration calorimetry measurements revealed a broad and tunable range of binding affinities across these

interaction modules, with no detectable non-specific binding to scaffold components. Within the coiled-coil class, affinities spanned nearly five orders of magnitude, with P3–P4 exhibiting the highest affinity (K_d = 5.4 nM), followed by P5–P6 (K_d = 39.4 nM), P13f–P14f (K_d = 0.94 μ M) (Fig. 5.11), and S3h–S4h showing markedly weaker binding (K_d = 340.3 μ M). Similarly, CL9–IM2 variants displayed graded binding strengths, ranging from high affinity for CL9–IM2_NVRT (K_d = 5.3 nM) to intermediate for CL9–IM2_WT (K_d = 116.7 nM) and low micromolar affinity for the attenuated mutant CL9–IM2_V37A (K_d = 3.86 μ M) (Fig. 5.12).

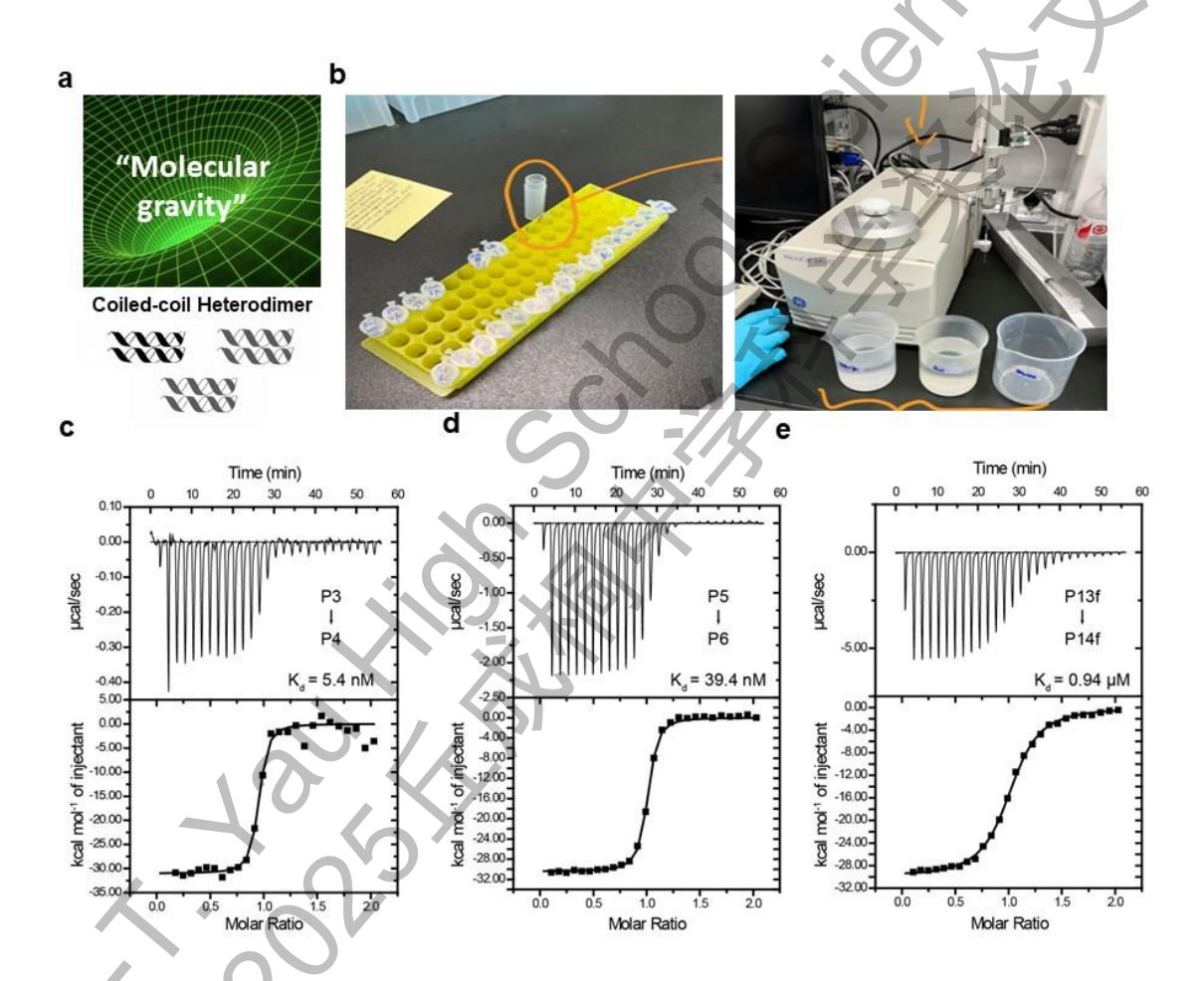


Fig. 5.11: Binding affinity measurements of coiled-coil heterodimer pairs.

- (a) Design molecular gravity: coiled-coil heterodimer linker pair.
- (b) The above images showing the ITC assay procedure.
- (c) ITC-based measurements of the binding affinities between heterodimer coiled-coil P3 and P4. 30 μM P3 was titrated into 3 μM P4. The fitted dissociation constant is 5.4 nM.
- (d) ITC-based measurements of the binding affinities between heterodimer coiled-coil P5 and P6. 200 μM P5 was titrated into 20 μM P6. The fitted dissociation constant is 39.4 nM.
- (e) ITC-based measurements of the binding affinities between heterodimer coiled-coil P13f and P14f. 500 μ M P13f was titrated into 50 μ M P14f. The fitted dissociation constant is 0.94 μ M.

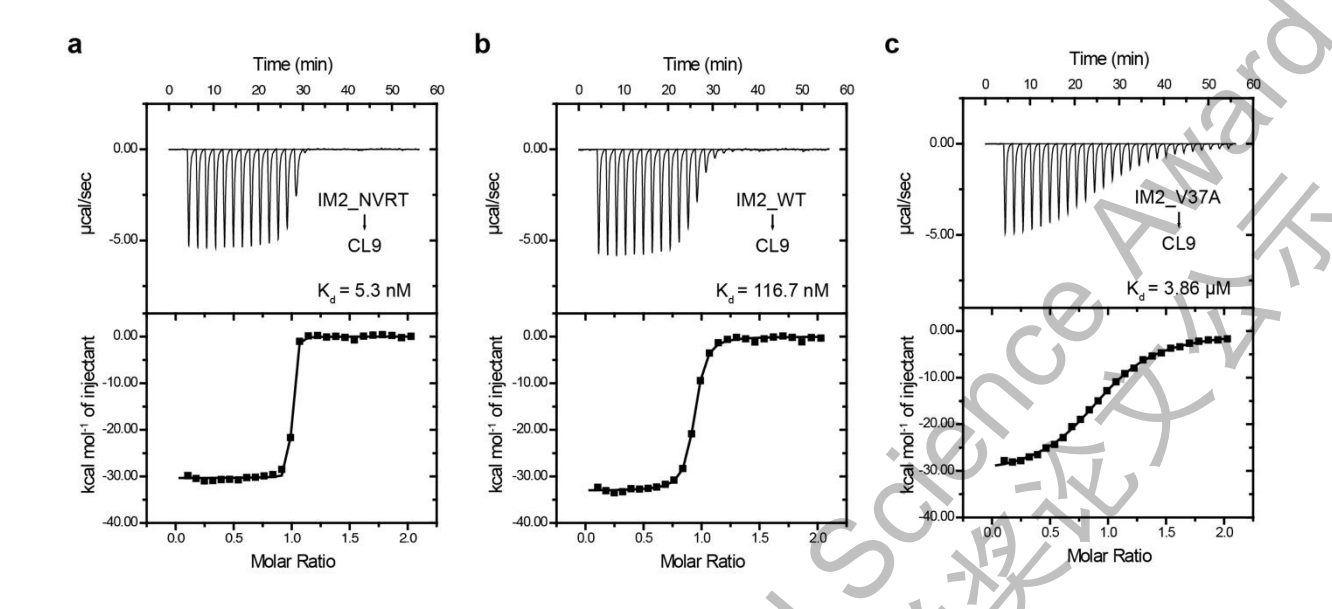


Fig. 5.12: Binding affinity measurements of Immunity2 (IM 2) to Colicin E9 (CL9).

- (a) ITC-based measurements of the binding affinities between IM2_NVRT and CL9. 500 μ M IM2_NVRT was titrated into 50 μ M CL9. The fitted dissociation constant is 5.3 nM.
- (b) ITC-based measurements of the binding affinities between IM2_WT and CL9. 500 μ M IM2_WT was titrated into 50 μ M CL9. The fitted dissociation constant is 116.7 nM.
- (c) ITC-based measurements of the binding affinities between IM2_V37A and CL9. 500 μ M IM2_V37A was titrated into 50 μ M CL9. The fitted dissociation constant is 3.86 μ M.

Gravitational Fields	Linker Pairs	Туре	Affinity	Functions
Type1 Heterodimeric Molecular gravity Coiled-Coil		P3–P4	5.4 nM	homogenous phase
	P13f–P14f	0.94 µM	phase-in- phase	
		S3h–S4h	340.3 µM	phase-to- phase
Type2 Molecular gravity		CL9-IM2_NVRT	5.3 nM	homogenous phase
	CL9-IM2	CL9-IM2_WT	116.7 nM	phase-in- phase
		CL9-IM2_V37A	3.86 µM	phase-in- phase

Table 5: Binding affinity of heterodimeric coiled-coil peptides and colicin E9 DNase (CL9)–Immunity 2 (IM2) Complex.

When introduced as synthetic linkers bridging orthogonal condensates, these differential affinities could result in distinct interfacial organization. High-affinity linkers (e.g., P3-P4 or IM2_WT) promote stable, long-lived molecular interaction events (e.g., CL9-IM2_WT, or P13f-P14f). Weak-affinity linkers (e.g., S3h-S4h or CL9-IM2_V37A) mediated highly transient, low-occupancy condensate contacts, allowing condensates to remain largely independent. Furthermore, by varying the relative abundance of condensate scaffolds conjugated to linker pairs, the strength and extent of interactions between orthogonal condensates can be quantitatively modulated. Collectively, this affinity-tunable interaction landscape constitutes a modular framework for programming synthetic condensate communication, where linker strength precisely

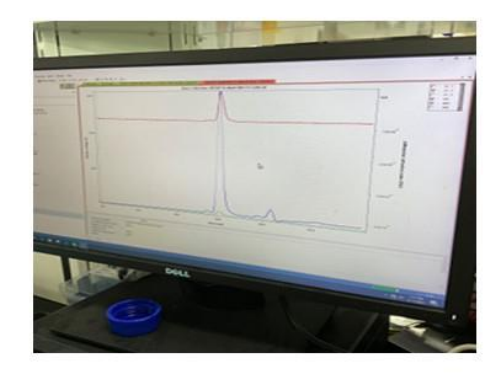
governs the stability, reversibility, and responsiveness of interfacial rewiring between orthogonal biomolecular condensate systems.

5.4 The Strength of the Gravitational Field Matters: Linker Strength Controls Scaffold Complex Formation

First, I tested the basic properties of my molecular 'planets' (like their size) and the strength of their 'gravity fields' individually. Now, I want to see if linking these planets with different gravitational strengths can create a stable system. This will give us the foundation we need for the next stage of design. So to evaluate whether the fusion of synthetic linker pairs facilitates the formation of stable complexes between otherwise non-interacting condensate scaffolds, I generated a series of chimeric constructs in which different linker pairs were covalently attached to RBP_(SH3)3 and (SIM)10 scaffolds. The interaction behavior of these modified scaffolds was analyzed using SEC-MALS. This approach enabled simultaneous assessment of complex formation by examining alterations in the elution profiles—specifically, the position and shape of chromatographic peaks—as well as by determining the fitted molecular weight (Mw) of each peak to infer the stability of potential heterodimeric complexes.

For the heterodimeric coiled-coil linker pairs, clear evidence of stable complex formation was obtained for scaffold pairs fused with the high-affinity linker P3–P4 (Kd = 5.4 nM). In this case, SEC-MALS profiles exhibited a pronounced shift of the elution peak toward earlier retention volumes, accompanied by a fitted molecular weight that closely matched the expected heterodimeric complex, demonstrating strong and persistent inter-scaffold association (Fig. 5.13a). Similarly, fusion with the intermediate-affinity P13f–P14f linker (Kd = 0.94 µM) resulted in detectable complex formation. Although the elution peak shift was less pronounced than for P3–P4, the increase in fitted molecular weight indicated the formation of stable heterodimeric assemblies under the experimental conditions (Fig. 5.13b). By contrast, the weakest coiled-coil pair, S3h–S4h (Kd = 340.3 µM), failed to produce a comparable effect. Elution profiles for S3h–S4h-linked scaffolds overlapped almost entirely with those of the individual scaffolds analyzed separately, and only a marginal increase in fitted molecular weight was observed (Fig. 5.13c), suggesting that this low-affinity linker was insufficient to promote detectable complex formation via SEC-MALS.

а





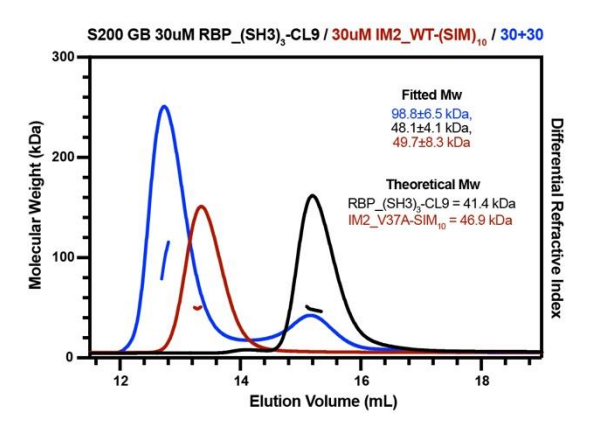
S200 GB 60uM RBP_(SH3)_x-P3 / 60uM P4-(SIM)₁₀ / 60+60

Fitted Mw
77.226.3 kDa,
407.45 k

Fig. 5.13: Complex formation between coiled-coil heterodimer fused scaffold proteins.

- (a)The above images demonstrating the SEC-MALS assay procedure.
- (b) SEC-MALS assay result showing that RBP_(SH3)3-P3 formed a stable complex with P4-(SIM)10.
- (c) SEC-MALS assay result showing that RBP_(SH3)₃-P13f formed a stable complex with P14f-(SIM)₁₀.
- (d) SEC-MALS assay result showing that there was almost no complex formation between RBP_(SH3) $_3$ -S3h and S4h-(SIM) $_{10}$

a b



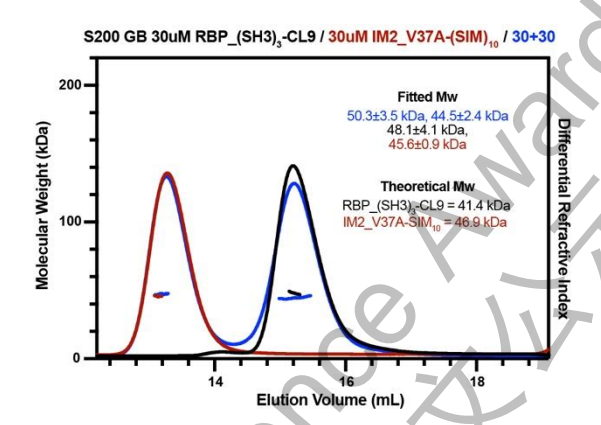


Fig. 5.14: Complex formation between IM2 and CL9 fused scaffold proteins.

- (a) SEC-MALS assay result showing that RBP_(SH3)₃-CL9 formed a stable complex with IM2_WT-(SIM)₁₀.
- (b) SEC-MALS assay result showing that there was almost no complex formation between RBP_(SH3)3-CL9 and IM2_V37A-(SIM)10.

Analysis of the second linker class, based on the CL9–IM2 interaction, yielded similar affinity-dependent behavior. Fusion of the high-affinity CL9–IM2_WT pair (Kd = 116.7 nM) to the scaffold proteins produced a distinct shift in the SEC elution profile, along with a fitted molecular weight consistent with the stoichiometry of a stable heterodimeric complex, indicating successful bridging of orthogonal scaffolds. In contrast, the relatively low-affinity variant CL9–IM2_V37A (Kd = 3.86 μ M) exhibited only minor alterations in both elution volume and molecular weight, suggesting that complex formation was weak and largely transient under the tested conditions.

Taken together, these SEC-MALS analyses demonstrate that synthetic linker-mediated complex formation between orthogonal condensate scaffolds is strongly dependent on the intrinsic binding affinity of the linker pair. High- and intermediate-affinity linkers, such as P3–P4, P13f–P14f, and CL9–IM2_WT, reliably facilitated the assembly of discrete heterodimeric complexes that were stable enough to be resolved by SEC-MALS. In contrast, low-affinity linkers like S3h–S4h and CL9–IM2_V37A were largely ineffective at bridging scaffolds, leading to minimal or no stable complex formation. These findings highlight the importance of linker affinity in programming scaffold interactions.

5.5 Simulate the Orbital Paths of Planets by Assembling "Molecular Planet and Gravity": Linker Affinity and Amount Determines Condensate Morphology

In space, a planet's gravity depends on its mass and the gravity of nearby planets. Similarly, I have to test different combinations of my molecular planets and gravities to see what happens. That's how we'll figure out how to design a reliable control system. To do this, first I systematically investigate how the affinity and abundance of synthetic linkers dictate the higher-order organization of multi-phase condensates, I varied both the binding strength and stoichiometry of linkers between the orthogonal condensate scaffolds (Fig. 5.15a, b). Across a broad range of interaction strengths, I observed that linker parameters not only influence condensate association but also define distinct structural architectures within multi-phase assemblies.

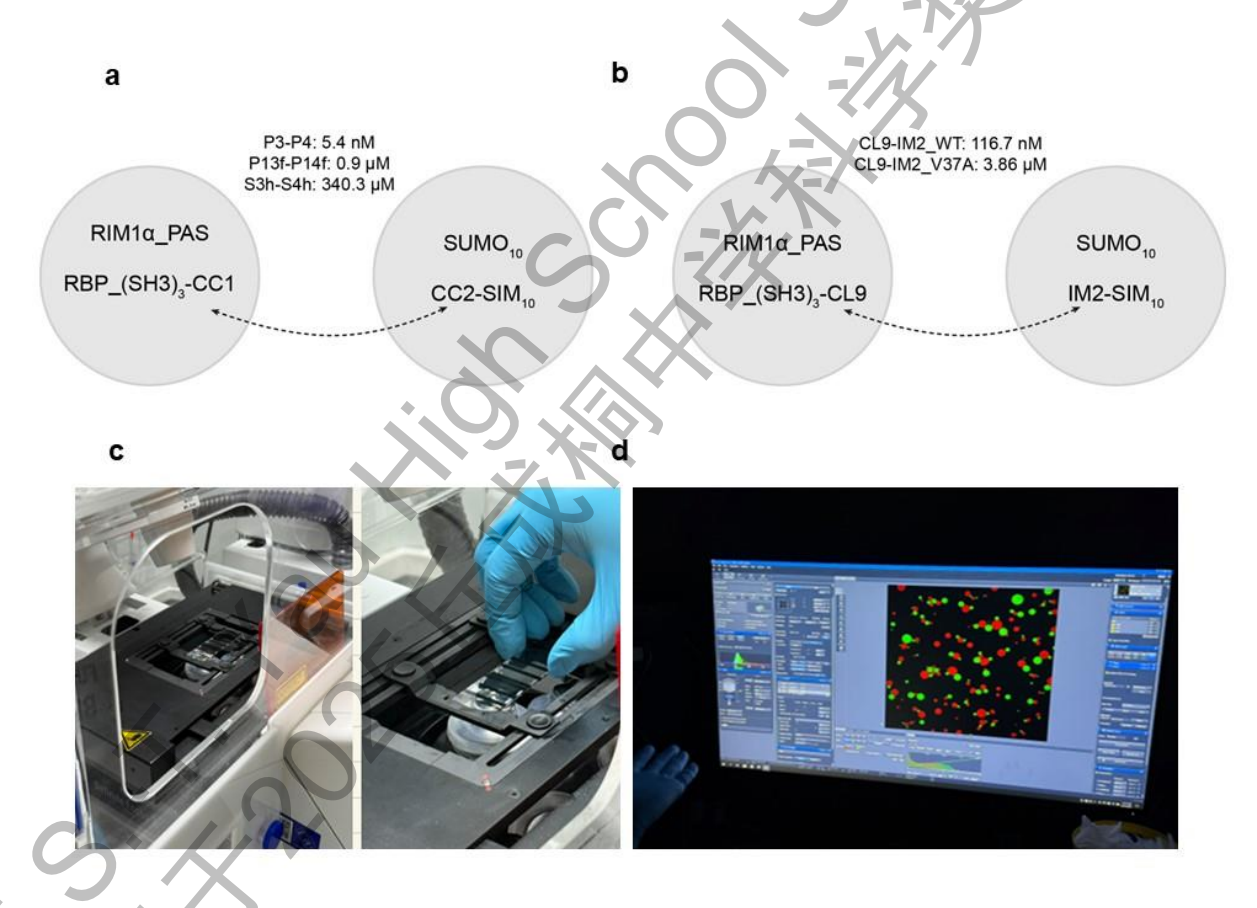


Fig. 5.15: Schematic diagram showing the strategy to create multi-phase condensate.

- (a) Schematic diagram showing the constructs for linking orthogonal condensates using heterodimer coiled-coils. CC1:P3, P13f and S3h; CC2: P4, P14f and S4h.
- (b) Schematic diagram showing the constructs for linking orthogonal condensates using CL9-IM2 interaction.
- (c-d) Image shows the confocal imaging procedure of multiple condensates formed by LLPS

When high-affinity linker pairs were utilized, exemplified by P3–P4 (Kd = 5.4 nM), the resulting orthogonal condensates formed compact, strongly interpenetrated assemblies in which the phase boundary between droplets became largely obscured. This state reflected persistent and robust molecular bridging that effectively collapsed the interface, giving rise to fused multi-component condensates lacking clear spatial segregation (Fig. 5.16).

By contrast, intermediate-affinity pairs, such as P13f–P14f (Kd = $0.94~\mu$ M), CL9–IM2_WT (Kd = 117~nM), and CL9–IM2_V37A (Kd = $3.86~\mu$ M), reproducibly promoted the emergence of "phase-in-phase" configurations (Fig. 5.16, 17). In these multilayered architectures, one condensate was completely enclosed within another, maintaining distinct internal phase boundaries. These nested assemblies illustrate how partial miscibility, coupled with moderately strong but non-saturating bridging, can reorganize droplets into hierarchically layered structures, enabling compartmentalization of different biochemical environments within a single larger entity.

At the lowest binding affinity examined, represented by the S3h–S4h pair (Kd = $340.3 \mu M$), condensates primarily exhibited "phase-to-phase" organizations with curved, well-defined interfaces (Fig. 5.15). In this regime, droplets remained largely immiscible yet stably adhered side by side, retaining sharp and persistent boundaries. Such configurations allowed only limited molecular exchange across phases while preserving close proximity, indicating that weak linkers are insufficient to drive engulfment but can nonetheless facilitate adhesion and ordered droplet arrangements.

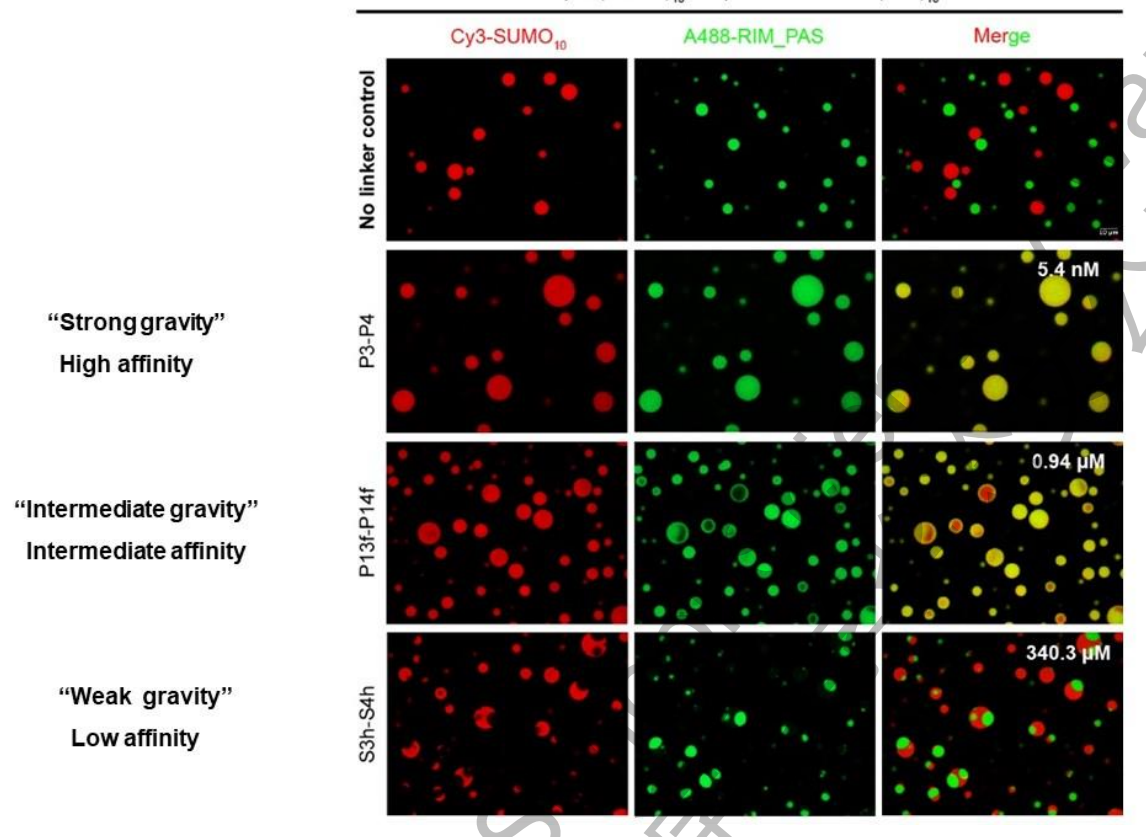
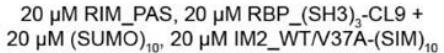


Fig. 5.16: Multi-phase phase-to-phase condensates induced by coiled-coil heterodimer interaction.

Confocal fluorescence images showing the morphology of the 2 orthogonalcondensates in which heterodimer coiled-coils was fused to the scaffold proteins to act as the linker. The binding affinities between the heterodimer coiled-coils were label in white on the upper right of the merged images.



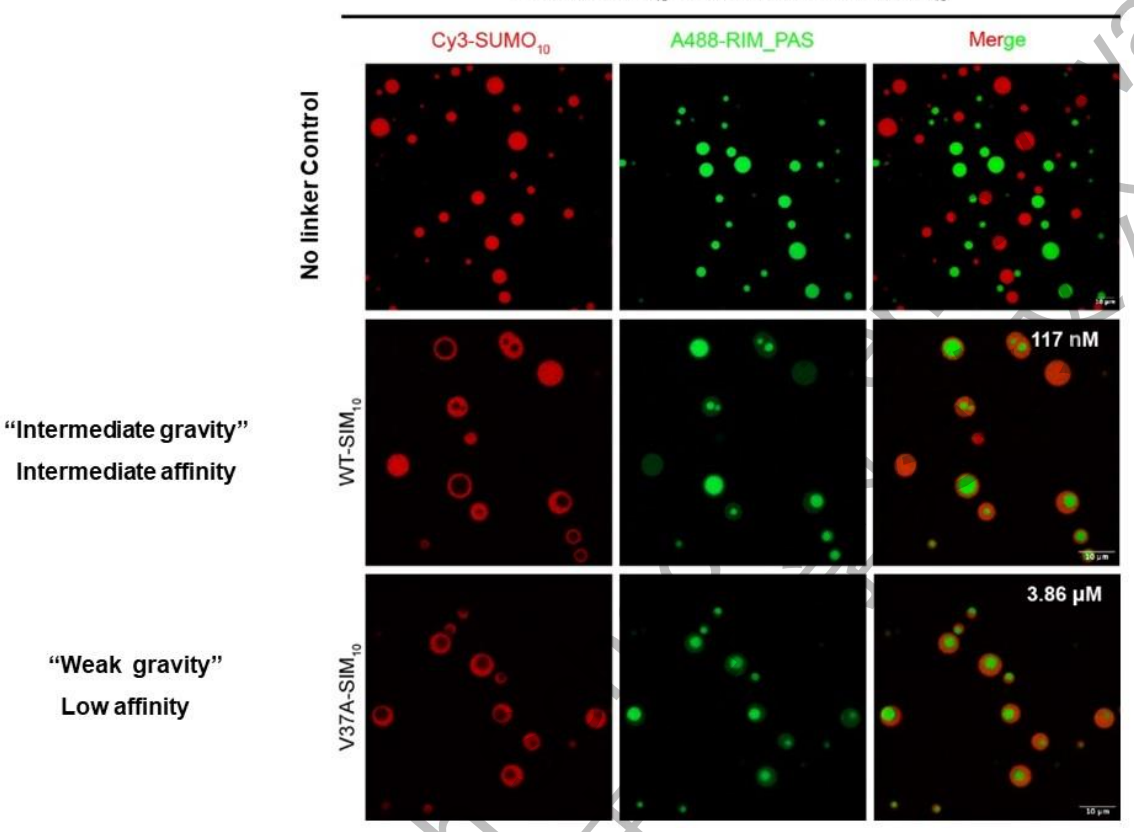


Fig. 5.17: Multi-phase phase-in-phase protein condensates induced by IM2 and CL9 interaction.

Confocal fluorescence images showing the morphology of the 2 orthogonal condensates in which CL9 and IM2 was fused to the scaffold proteins to act as the linker. The binding affinities between CL9 and IM2_WT or IM2_V37A were label in white on the upper right of the merged images.

Linker abundance further tuned these multi-phase condensate structural outcomes. Reducing the proportion of scaffold proteins conjugated to linkers to 10% markedly diminished condensate connectivity, resulting in sporadic, incomplete contact points and largely separated droplets. For the high affinity P3–P4 interaction, the decreased amount changed the condensates to "phase-to-phase" structure (Fig. 5.18). For the other lower affinity conditions, multi-phase architectures were formed with contact, and condensates maintained independent with minimal interfacial interactions (Fig. 5.18,19).

Collectively, these results demonstrate that the structural organization of multiphase condensates can be finely programmed by adjusting both the binding affinity
and relative abundance of synthetic linkers. Through this dual parameter control, it is
possible to engineer a continuum of higher-order condensate architectures ranging
from fully interpenetrated droplets to nested phase-in-phase structures or discrete
side-by-side assemblies, providing a versatile framework for constructing synthetic,
spatially organized biomolecular condensates.

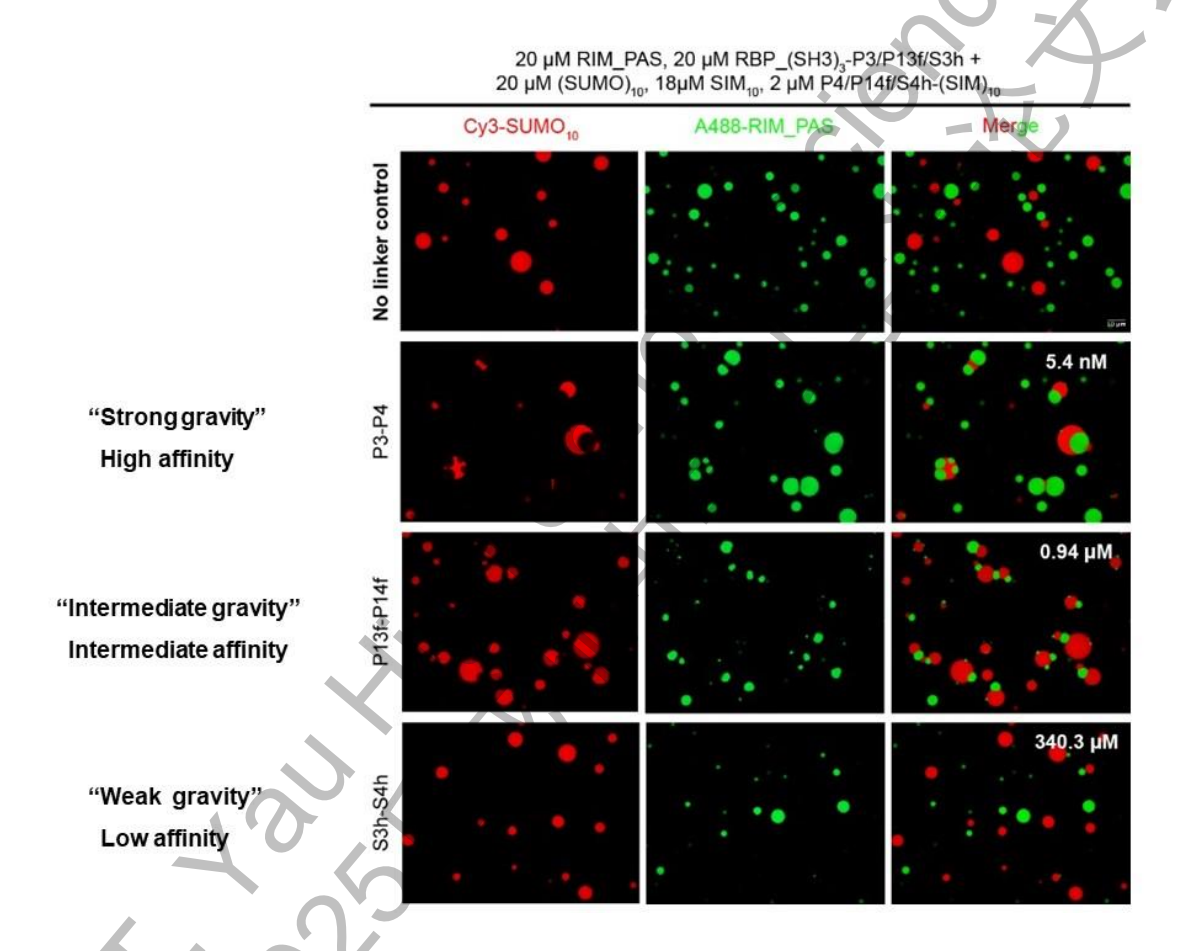


Fig. 5.18: Lowering the coiled-coil heterodimer linker amount alters the multi-phase condensate morphology.

Confocal fluorescence images showing the morphology of the 2 orthogonal condensates in which heterodimer coiled-coils was fused to the scaffold proteins to act as the linker. The amount of the P4/P14f/S4h fused (SIM)₁₀ was descreased to 2 μ M.



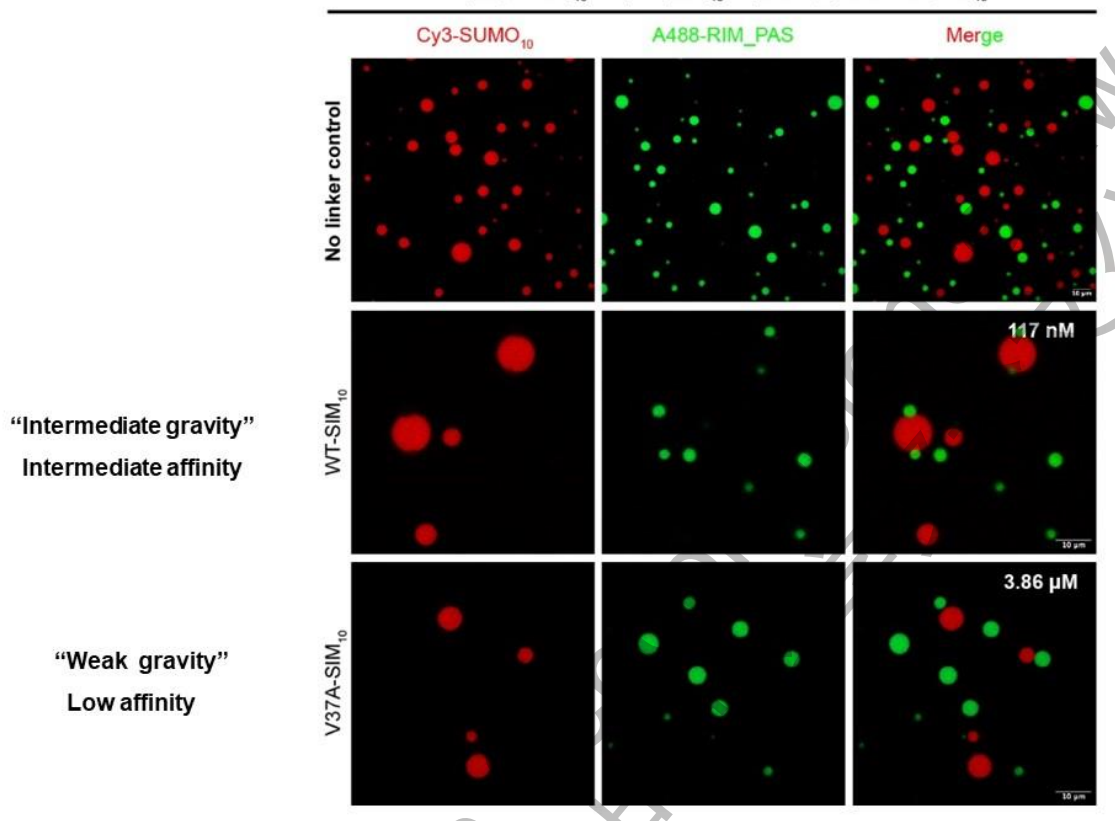


Fig. 5.19: Lowering IM2 and CL9 interaction pair amount deplete the phase-in-phase condensate.

Confocal fluorescence images showing the morphology of the 2 orthogonal condensates in which CL9 and IM2 was fused to the scaffold proteins to act as the linker. The amount of the IM2_WT or IM2_V37A fused (SIM) $_{10}$ was decreased to 2 μ M.

5.6 Testing the Controllable Operating System of an "Artificial Planet": Programmable induction of Phase-in-Phase Architectures in Cells

Controlling how planets move is way too hard and unrealistic for someone like me. But what if I could control the shape and behaviour of condensates at the molecular level? That's the most exciting part of my research—it lets me satisfy that desire to design a system and control celestial motion, just in a microscopic universe. Having established the fundamental physical principles governing linker-mediated assembly using purified, well-defined *in vitro* systems, I next sought to determine if these principles are robust enough to operate within the complex and dynamic environment of a living mammalian cell. A direct translation of the RIM/RBP or SUMO/SIM systems into cells presents potential challenges; the overexpression of highly multivalent, artificial scaffolds like (SUMO)₁₀ and (SIM)₁₀ can impose a significant protein expression burden, potentially triggering cellular stress responses, protein degradation pathways, or other off-target effects that could confound the interpretation of condensate behavior.

To achieve easier and more stable artificial manipulation of planetary motion, I have selected a classic model molecular system here. In other word, to reduce these potential artifacts and test the biological universality of my design strategy, I therefore transitioned to a different pair of orthogonal scaffolds known for their robust and predictable phase separation behavior in mammalian cells: DDX4 and LAF1. This strategic switch allows us to "graft" the linker-based control mechanism, validated with high precision *in vitro*, onto a more biologically relevant chassis. This two-stage approach enables us to first isolate the core physical chemistry of the system and then validate its functional application in a physiological context, bridging the gap from a physical model to a viable synthetic biology tool.

Therefore, to explore whether synthetic linkers can be used to manipulate condensate—condensate interactions and promote multi-phase organization in living cells, I reconstituted two orthogonal condensate systems in HeLa cells and examined their spatial reorganization upon expression of a bridging-free linker molecule. The first condensate scaffold was based on pmCherry-DDX4-SAMWT²⁴, while the second scaffold consisted of pmEGFP-LAF1_RGG-(S1h-S3h)3-(S2h)3(S4h)3¹⁴, which would independently formed microscopically visible condensates when expressed in the same cell. Leveraging the well-characterized interaction between PSD-95_GK and its

specific nanobody PSD-95.FingR (FR)²⁵, I established a two-step synthetic bridging strategy. I first fused CL9 to LAF1_RGG-(S1h-S3h)₃-(S2h)₃-(S4h)₃, enabling potential recruitment via IM2-based interactions, and fused PSD-95_GK to DDX4-SAMWT to provide a cognate binding site for FingR. Subsequently, the Xlone Tet-On expression system ²⁶ was used to inducibly express miRFP-IM2-FR as a freely diffusible, bridge-like linker after both orthogonal condensates had independently assembled in the cells. This design allowed IM2 to bind the CL9-modified condensates, while FR binding the PSD-95_GK-fused scaffold, thus bridging the two condensate populations without direct scaffold modification or covalent fusion (Fig. 5.20). I first co-expressed the IM2-FR bridge linker with the two condensate scaffold proteins in hela cell, respectively. The addition of doxycycline induced the expression of IM2-FR and the bridge linker co-localized with both the two scaffold proteins, respectively (Fig. 5.21a,b). Then these two scaffold systems were verified to be orthogonal, showing no detectable fusion or spontaneous intermixing in the absence of engineered linkers (Fig. 5.22a).

I co-expressed the two scaffolds with the linker IM2-FR. After the scaffold proteins expressed for 8 hours, I confirmed the formation of orthogonal condensates by live cell imaging. Then I added doxycycline to induce the expression of IM2-FR. Upon induced expression of IM2-FR, I observed a striking reorganization of the two condensate types, leading to the emergence of a phase-in-phase multiphase architecture. Specifically, condensates containing pmCherry-GK-DDX4-SAMWT formed the outer shell, while the pmEGFP-CL9-LAF1_RGG-(S1h-S3h)3-(S2h)3(S4h)3 condensates were fully engulfed within this outer condensate layer, forming nested structures with well-defined phase boundaries (Fig. 5.22b). This reorganization was absent in control cells without IM2-FR expression (Fig. 5.22a), confirming that synthetic bridging was necessary to establish stable interfacial interactions between otherwise orthogonal condensates.

These findings demonstrate that programmable condensate wetting and multiphase assembly can be achieved in heterologous mammalian cells by introducing a bridge-free synthetic linker. Furthermore, they show that cellular phase organization can be rationally rewired post-condensate formation, enabling dynamic control over the spatial hierarchy and compartmentalization of synthetic biomolecular condensates in vivo.

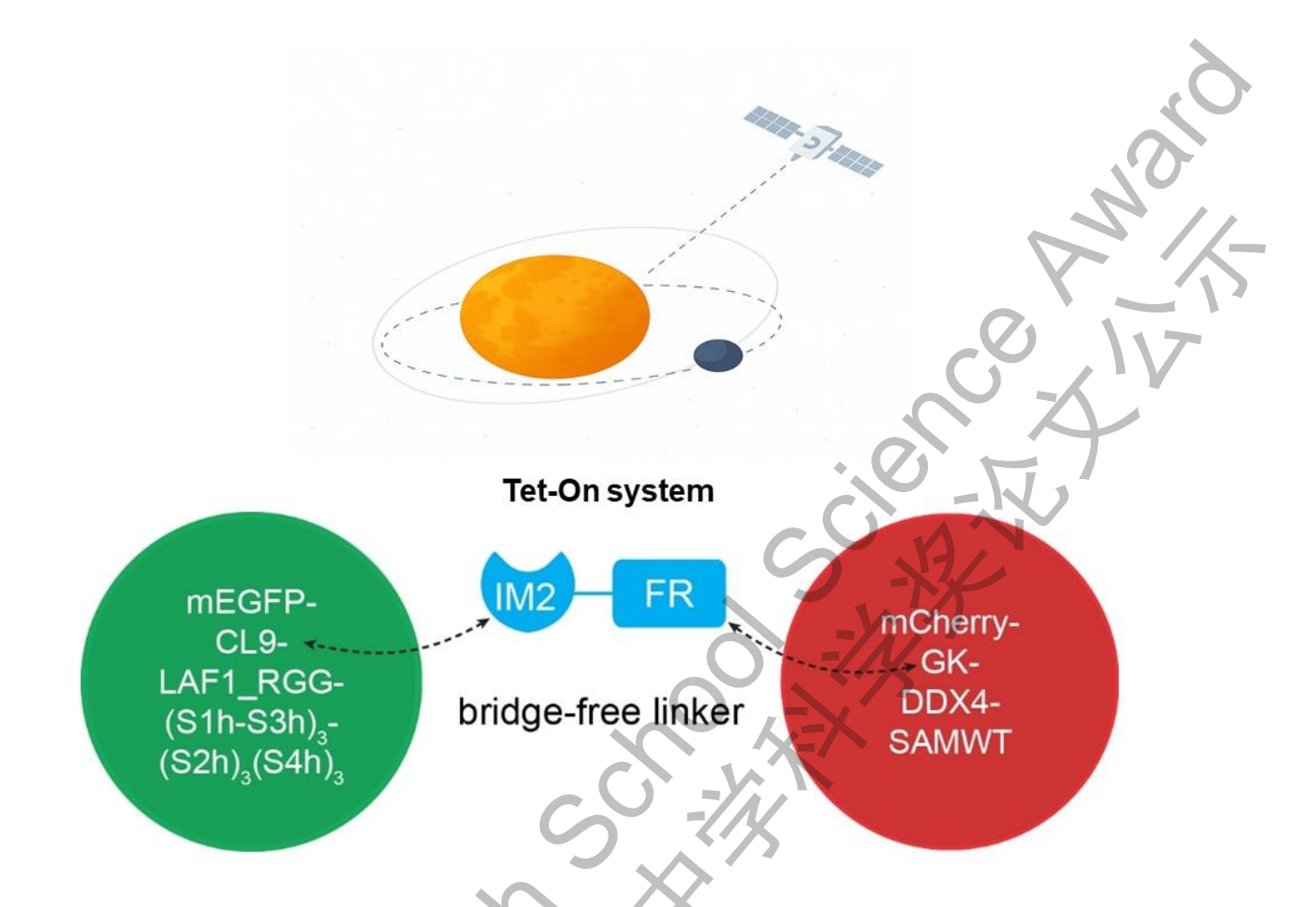


Fig. 5.20: Schematic diagram showing the strategy to induce the free linker as a bridge between two orthogonal condensates in heterologous cells. Just like design an operating system to control an artificial planet in universe.

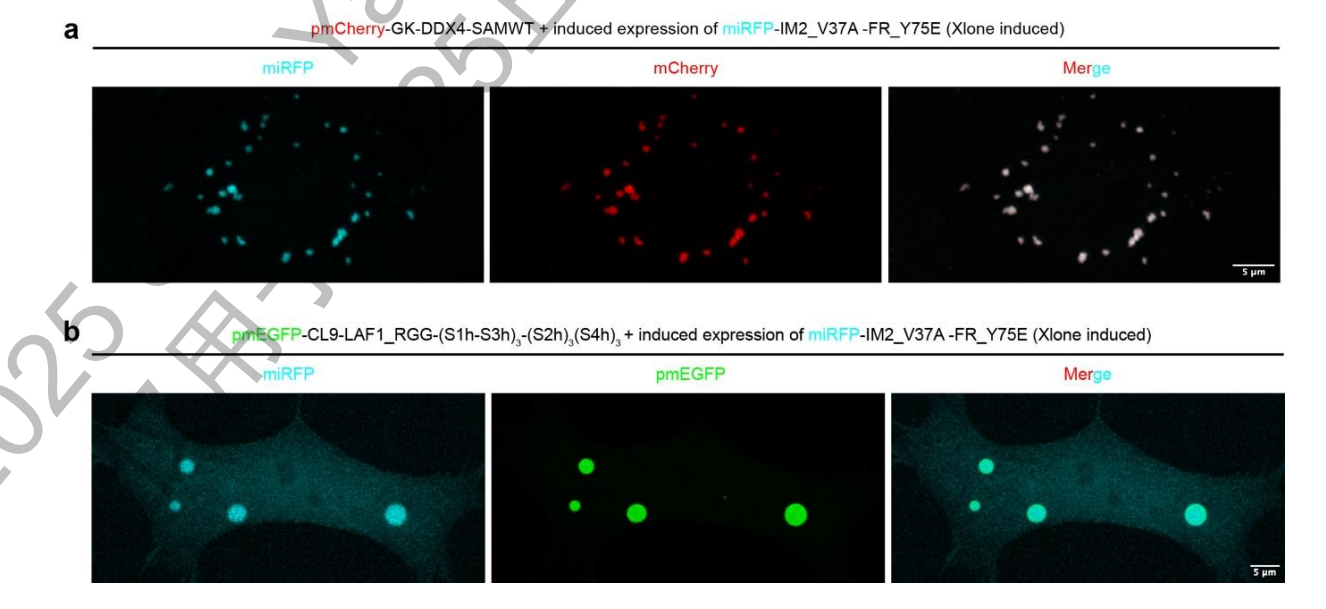


Fig. 5.21: The free linkers express after doxycycline addition and colocalize with the condensates.

(a) Confocal fluorescence images of one representative Hela cell with condensate scaffold protein pmCherry-GK-DDX4-SAMWT co-expressed with the free linker to show that they are co-localized. (b) Confocal fluorescence images of one representative Hela cell with condensate scaffold protein pmEGFP-CL9-LAF1_RGG-(S1h-S3h)3-(S2h)3(S4h)3 co-expressed with the free linker to show that they are co-localized.

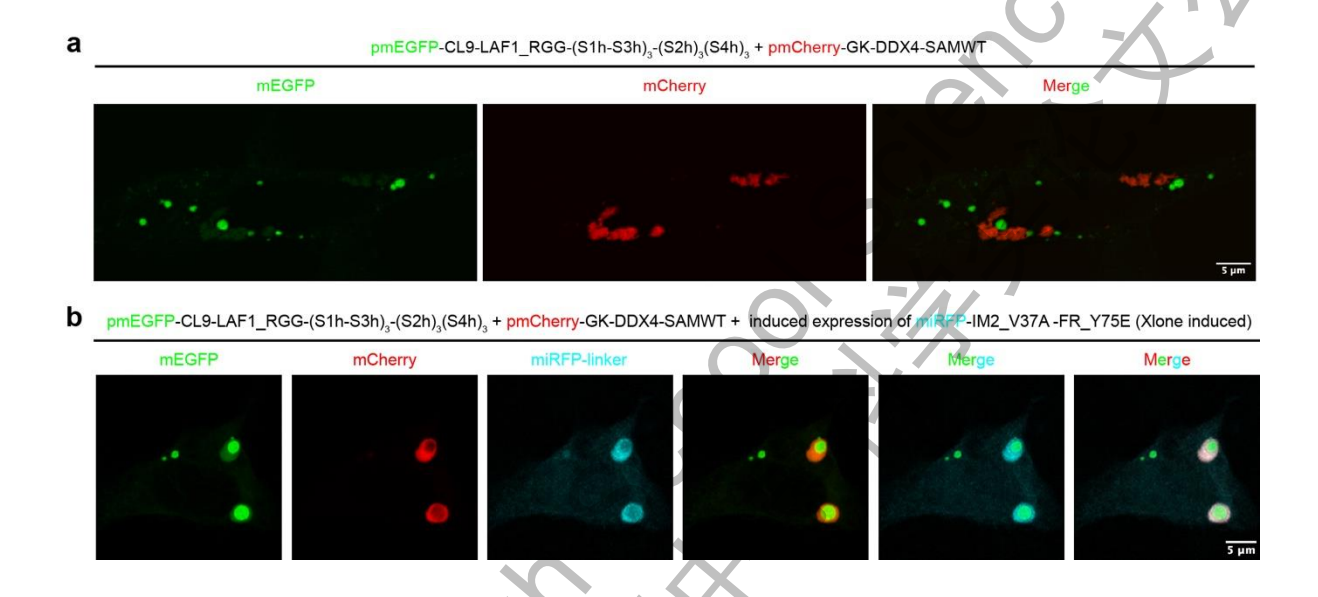


Fig. 5.22: Induced expression of the free linker in heterologous cells generates phase-inphase condensates.

- (a) Confocal fluorescence images of one representative Hela cell with two kinds of condensate scaffold proteins co-expressed to show that they are not co-localized.
- (b) Confocal fluorescence images showing the multi-phase condensate morphology in one representative Hela cell with condensate scaffold proteins and the free linkers co-expressed.

6. Summary

In this study, I investigated two condensates formed by multivalent interaction between multi-domain scaffolds. Using the FRAP assay, I confirmed the molecular dynamics of the condensates. I identified specific interaction pairs (heterodimer coiledcoils and Colicin E9:CL9/Immunity2:IM2) as the linker between orthogonal networked condensates. Using this method, I successfully built multi-phase condensates with two main types of organization. One is called "phase-in-phase," where one droplet is completely surrounded by another, like a bubble inside a bigger bubble. The other is "phase-to-phase," where two droplets sit next to each other but don't mix, keeping clear boundaries. I observed these structures both in vitro using purified proteins, and also in heterologous cells (in vivo) that I modified to express the scaffold proteins²⁰. These studies demonstrate that I can design the layered internal condensate structure through engineering the interaction and interface between macromolecules. This also showed that my approach is stable and works in different biological settings. The designer multi-phase condensates would be very useful for building synthetic organelles, controlling cellular metabolic activity, and even developing therapeutic delivery treatments. From a synthetic biology perspective, my approach offers several major benefits:

First, because the scaffolds are modular and orthogonal, I can combine different protein parts—like enzymes or signaling domains—within one organized condensate. This makes it possible to build membrane-less organelles that can be programmed to carry out specific tasks in cells.

Second, the multi-phase design helps control how molecules move between different reactions. For example, in enzyme pathways with multiple steps, placing each step in a different phase can trap unstable intermediates and prevent them from diffusing away or causing harm. This can improve the speed, efficiency, and safety of biochemical reactions.

Third, by physically separating different reactions into their own droplet phases, I can reduce unwanted crosstalk between pathways. This improves the accuracy and reliability of synthetic biological systems, allowing us to better control what happens inside a cell.

7. Discussion

From Cosmic Order to Cellular Self-Organization: Gravity and multivalent interaction

My interest in astronomy is not only about looking at the stars—it also helps me think about how order can appear in nature. When I take photos of galaxies and nebulae, I often wonder how those huge systems form beautiful patterns out of so much chaos. Later, when I studied biology, I realized that something similar happens inside our cells. Just like stars and planets form through gravity, proteins and molecules in a cell can come together and organize themselves through forces at the molecular level.

This connection between the large and the small inspired me to think across different scales. When I first saw small dark droplets forming in a mix of olive oil and vinegar, they looked to me like tiny planets floating in space. Later, when I learned about liquid—liquid phase separation (LLPS) and saw droplet-like organelles inside cells, I felt as if I had found the "molecular version" of the universe. Both systems—cosmic and cellular—follow simple physical rules that turn disorder into structure.

Thinking like an astronomer helped me design biological experiments in a new way. I began to see the cell as a little universe where molecules move and interact like stars under gravity. By studying how molecular "forces" affect the shape and behavior of protein condensates, I realized that I could apply the same ideas used to explain planetary motion to understand how life organizes itself inside cells. For me, astronomy is more than a hobby—it is a way to train my curiosity and imagination. It reminds me that the same laws of nature shape everything, from galaxies to cells. Looking at the stars helped me see the hidden universe within living things, showing that both the sky above and the life within us are built on the same beautiful principles of self-organization.

Transitioning from *In Vitro* Principles to *In Vivo* Validation: Programmable Multiphase Condensate

Having established the fundamental physical principles governing linker-mediated assembly using purified, well-defined *in vitro* systems, I next sought to determine if these principles are robust enough to operate within the complex and dynamic environment of a living mammalian cell. A direct usage of the RIM/RBP or

SUMO/SIM systems into cells presents potential challenges; the overexpression of highly multivalent, artificial scaffolds like (SUMO)₁₀ and (SIM)₁₀ can impose a significant protein expression burden, potentially triggering cellular stress responses, protein degradation pathways, or other off-target effects that could confound the interpretation of condensate behavior. To mitigate these potential artifacts and test the biological universality of our design strategy, I therefore transitioned to a different pair of orthogonal scaffolds known for their robust phase separation behavior in mammalian cells: intrinsically disorder sequences DDX4 and LAF1 combined with oligomerization domain or tandem repeats of coiled-coils.

In this heterollogous cell experiments, I engineered an innovative inducible, bridge-free linker strategy. This design offers two critical advantages in a complex cellular environment. First, it circumvents the technical challenge of matching the expression levels of two separate fusion proteins. Second, and more importantly, it introduces invaluable temporal control. By using a doxycycline-inducible system, I could first allow the orthogonal condensates to form independently, establishing a baseline state. I then triggered the expression of the bridging linker, allowing us to observe the dynamic reorganization into a phase-in-phase architecture in real-time within the same cell. This design provides a powerful internal control, offering definitive causal evidence for the linker's function and better mimicking physiological processes where signaling molecules are produced on-demand to mediate interactions between cellular compartments.

A Physical Model for Programmable Multi-Phase Architectures: Soft Matter Physics

The observed correlation between linker affinity and multi-phase morphology can be rationalized through the classical physics of interfacial tension. A system containing two immiscible condensate phases (α and β) immersed in a dilute aqueous phase (S) will adopt a configuration that minimizes its total free energy. This configuration is dictated by the balance of three interfacial tensions: $\gamma\alpha S$, $\gamma\beta S$, and $\gamma\alpha\beta T$ he tendency of one phase (e.g., β) to spread over another (α) is quantified by the spreading coefficient, $S=\gamma\alpha S-(\gamma\beta S+\gamma\alpha\beta)$. When S<0, the system favors minimizing the α - β contact area, resulting in partial wetting (a stable contact angle) or complete demixing. When S>0, it is energetically favorable for phase β to completely envelop phase α , a

phenomenon known as complete wetting. I propose that my engineered linkers function as programmable "molecular surfactants" that specifically adsorb at the α - β interface and modulate its interfacial tension, $\gamma\alpha\beta$. The affinity and concentration of these linkers directly control the magnitude of this reduction. This model provides a powerful physical explanation for my experimental results (table 5):

Very Low Affinity (e.g., S3h-S4h, CL9–IM2_V37A): In the absence of effective linkers, γαβ is high, yielding a negative spreading coefficient (S<0). This results in the observed demixed or "phase-to-phase" structures, where droplets maintain distinct boundaries and either do not touch or form a stable, partial-wetting interface.

Intermediate Affinity (e.g., P13f-P14f, CL9-IM2 WT): Linkers with intermediate affinity are sufficiently strong to populate the interface and significantly lower $\gamma\alpha\beta$. This reduction is enough to drive the spreading coefficient positive (S>0), triggering a wetting transition. Consequently, the system reconfigures to form the energetically favorable "phase-in-phase" architecture, where one condensate is fully engulfed by the other.

Very High Affinity (e.g., P3-P4, CL9-IM2_NVRT): With extremely high-affinity linkers, the interfacial tension $\gamma\alpha\beta$ is reduced so drastically that it approaches zero. The thermodynamic distinction between the two phases is effectively erased, eliminating the driving force for demixing and leading to the fusion of the two condensates into a single, homogenous phase.

This framework transforms our system from a set of empirical observations into a predictive platform. It demonstrates that by tuning a single molecular parameter—linker affinity—we can drive a biological system through a classic physical wetting transition, allowing us to rationally program the mesoscale architecture of synthetic organelles. Overall, my work presents a new way to design multiple, coexisting, membrane-less compartments inside cells, each with its own function. The strategies I developed here offer both the ideas and tools needed to build synthetic condensates with layered organization and tunable interfaces. This is a big step forward in turning the complex natural process of phase separation into a practical tool for synthetic biology. Looking ahead, engineering multi-phase condensates could become a core technology for many future applications, including improving metabolic pathways, controlling intracellular reactions, and even creating artificial, cell-like systems that use spatial organization to carry out advanced biochemical functions.

8. References

- Feng, Z., Chen, X., Wu, X. & Zhang, M. Formation of biological condensates via phase separation: Characteristics, analytical methods, and physiological implications. *J Biol Chem* **294**, 14823-14835 (2019).
- 2 Hyman, A. A., Weber, C. A. & Julicher, F. Liquid-liquid phase separation in biology. *Annu Rev Cell Dev Biol* **30**, 39-58 (2014).
- Dai, Y. *et al.* Programmable synthetic biomolecular condensates for cellular control. *Nat Chem Biol* **19**, 518-528 (2023).
- 4 Lafontaine, D. L. J., Riback, J. A., Bascetin, R. & Brangwynne, C. P. The nucleolus as a multiphase liquid condensate. *Nature Reviews Molecular Cell Biology* **22**, 165-182 (2021).
- Brangwynne, C. P. *et al.* Germline P granules are liquid droplets that localize by controlled dissolution/condensation. *Science* **324**, 1729-1732 (2009).
- 6 Alberti, S., Gladfelter, A. & Mittag, T. Considerations and Challenges in Studying Liquid-Liquid Phase Separation and Biomolecular Condensates. *Cell* **176**, 419-434 (2019).
- 7 Banani, S. F., Lee, H. O., Hyman, A. A. & Rosen, M. K. Biomolecular condensates: organizers of cellular biochemistry. *Nat Rev Mol Cell Biol* **18**, 285-298 (2017).
- 8 Li, P. *et al.* Phase transitions in the assembly of multivalent signalling proteins. *Nature* **483**, 336-340 (2012).
- 9 Cascarina, S. M., Elder, M. R. & Ross, E. D. Atypical structural tendencies among low-complexity domains in the Protein Data Bank proteome. *PLoS Comput Biol* **16**, e1007487 (2020).
- Gao, Y., Li, X., Li, P. & Lin, Y. A brief guideline for studies of phase-separated biomolecular condensates. *Nat Chem Biol* **18**, 1307-1318 (2022).
- Garabedian, M. V. *et al.* Designer membraneless organelles sequester native factors for control of cell behavior. *Nat Chem Biol* **17**, 998-1007 (2021).
- 12 Qian, Z. G., Huang, S. C. & Xia, X. X. Synthetic protein condensates for cellular and metabolic engineering. *Nat Chem Biol* **18**, 1330-1340 (2022).
- Baruch Leshem, A. *et al.* Biomolecular condensates formed by designer minimalistic peptides. *Nat Commun* **14**, 421 (2023).
- 14 Ramsak, M. *et al.* Programmable de novo designed coiled coil-mediated phase separation in mammalian cells. *Nat Commun* **14**, 7973 (2023).
- 15 Quinodoz, S. A. *et al.* Mapping and engineering RNA-driven architecture of the multiphase nucleolus. *Nature* **644**, 557-566 (2025).
- Lu, T. & Spruijt, E. Multiphase Complex Coacervate Droplets. *J Am Chem Soc* **142**, 2905-2914 (2020).
- 17 Wu, X. *et al.* RIM and RIM-BP Form Presynaptic Active-Zone-like Condensates via Phase Separation. *Mol Cell* **73**, 971-984 e975 (2019).
- Banani, S. F. *et al.* Compositional Control of Phase-Separated Cellular Bodies. *Cell* **166**, 651-663 (2016).
- Zeng, M. *et al.* Phase Transition in Postsynaptic Densities Underlies Formation of Synaptic Complexes and Synaptic Plasticity. *Cell* **166**, 1163-1175 e1112 (2016).
- 20 Zhu, S. *et al.* Demixing is a default process for biological condensates formed via phase separation. *Science* **384**, 920-928 (2024).
- 21 Chen, Y. *et al.* Phase separation instead of binding strength determines target specificities of MAGUKs. *Nat Chem Biol* (2025).

- Lebar, T., Lainscek, D., Merljak, E., Aupic, J. & Jerala, R. A tunable orthogonal coiled-coil interaction toolbox for engineering mammalian cells. *Nat Chem Biol* **16**, 513-519 (2020).
- Heidenreich, M. *et al.* Designer protein assemblies with tunable phase diagrams in living cells. *Nat Chem Biol* **16**, 939-945 (2020).
- Shen, Z. *et al.* Biological condensates form percolated networks with molecular motion properties distinctly different from dilute solutions. *Elife* **12** (2023).
- Gross, G. G. *et al.* Recombinant probes for visualizing endogenous synaptic proteins in living neurons. *Neuron* **78**, 971-985 (2013).
- 26 Randolph, L. N., Bao, X., Zhou, C. & Lian, X. An all-in-one, Tet-On 3G inducible PiggyBac system for human pluripotent stem cells and derivatives. *Sci Rep* **7**, 1549 (2017).

9. Acknowledgements

One of my hobby is astrophotography, I often visit the Shenzhen Observatory to capture the beauty of the night sky. The way nebulae and planets self-organize in the vast universe fascinates me. They seem to follow natural laws that bring order out of chaos. Initially, I was inspired by these small black droplet when I dipping my bread in olive oil and vinegar mixture at breakfast. This starting point that I try to know about the phenomena of liquid-liquid phase separation. Further, in my biology class, I was amazed to see something familiar inside cell compare to planets and nebuae in the universe. This similarity between the universe and the inside of a cell sparked a big question in my mind: could both follow the same self-organization principles. Inspired, I started reading more about LLPS and learned how it allows proteins and molecules to separate and gather inside cells without needing membranes, much like how gravity pulls matter together in space. These are all thanks to my parents, who provided me with the necessary equipment, often took me to visit observatories, and encouraged me to think across disciplines.

I began simple experiments in my school's synthetic biology lab. These experiments gave me a sense of how order can emerge in the microscopic world. At the beginning of this year I visited the Southern University of Science and Technology (SUSTech), where I had the chance to tour Professor Mingjie Zhang's lab. I learned about their research on membraneless organelles and a process called liquid-liquid phase separation (LLPS).Later, I contacted Professor Zhang, and he agree me to enter his the lab. He encouraged me to combine my cross-scale thinking with real scientific research. His team is now working on using synthetic biology to design programmable protein modules that can form controllable structures inside cells—like building planets, but on the molecular level. This is thanks to Shenzhen Middle School and my mentor, Dr. Hu, who provided me with the opportunity to visit cutting-edge university science laboratories and offered access to a synthetic biology lab for my initial explorations, allowing me to engage more closely with the frontiers of scientific research.

After entering the experiment, in addition to Prof. Zhang providing me with research ideas and answering my scientific questions, I encountered many difficulties during the specific laboratory procedures. I am especially grateful to Mr. Yan Chen for patiently teaching me the skills to perform biological experiments in a standardized

manner. One of the primary challenges I encountered was designing condensate linker interaction pairs that were orthogonal to the all the core scaffolds. The two condensates selected for *in vitro* study contains several protein domains and the linker interaction should be orthogonal to them all. To address this, I undertook a review of some literature, examining articles that reported well-characterized protein-protein interaction pairs with minimal cross-reactivity to related scaffold architectures, the selection of linkers in this section was also determined under the strong guidance of Mr. Yan Chen. By comparing reported binding affinities, structural features, and domain compositions from these studies, I identified candidate interaction pairs including the coiled-coils and the Colicin/Immunity with varying affinities that unlikely to interact with the scaffold sequences used in my work. These interaction modules were incorporated into scaffold designs and validated experimentally.

Generating the multi-phasic condensates also required significant protein production skill and learning how to purify the proteins involved. Of course, many of the high-quality purified proteins in this paper were provided by our laboratory. Under the guidance of an experienced senior lab member, there are quite a lot of detailed experimental techniques including protein purification, ITC assay, and size-exclusion chromatography, which required building technical expertise from the ground up. This process of skill acquisition was very important in transforming conceptual designs into experimentally validated multiphase condensate systems.

Finally, I would like to thank Prof. Zhang, Dr. Hu, and graduate student Mr. Yan Chen for their suggestions on revising my paper, without the selfless and dedicated guidance of them, I could never have completed this entire research report on my own. I am deeply grateful to all those who supported me in realizing the full journey of this research—from initial life inspiration to laboratory validation. As well as my parents for their all-round support. Without your help and encouragement, it would have been difficult for me to complete this research journey.

Personal CV:

Name:

Yihao Li

Education:

Shenzhen Middle School (9/2024-present)

Position and Award:

Shenzhen Middle School Animal Protection Society:

• The president (2025)

Shenzhen Middle School International Department Studio (SMSID Studio):

• The Cofounder (2025)

Canadian Chemistry Contest (CCC):

National Gold Award (top10%) (04/2025)

Shenzhen Middle School:

Merit Student (2025)

Shenzhen Experimental School:

Outstanding Graduate (top5%) (7/2024)

Shenzhen Experimental School:

Top 10 Science and Technology Award (04/2022)

National Wetland Nature Journal Program:

National Outstanding Work (09/2022)

Introduction to my mentor:

1, Chair Professor. Mingjie Zhang:

Introduction:

BSc (Fudan University, China); Ph.D. (University of Calgary, Canada); Member of Chinese Academy of Sciences; Founding Member of the Academy of Sciences of Hong Kong

Founding Dean, School of Life Sciences, Southern University of Science and Technology (SUSTech)

Prof. Mingjie Zhang obtained his bachelor's degree in chemistry from Fudan University, Shanghai in 1988, and his Ph.D. degree in Biochemistry in the University of Calgary, Canada in 1994. After a brief postdoctoral training in the Ontario Cancer Institute, Toronto, Canada, he established his own laboratory as an Assistant Professor in the Department of Biochemistry, Hong Kong University of Science and Technology (HKUST) in 1995. Before becoming to be the Founding Dean of School of Life Sciences at SUSTech, Prof Zhang was a Kerry Holdings Professor of Science, Senior Fellow of the Institute for Advanced Study, and Chair Professor in the Division of Life Science, HKUST.

Research Interests:

1. Biochemical and structural basis of important protein complexes in neural signal transduction.

Mechanisms of the generation and maintenance of neural cell polarity

Professional Experience:

2020-now Southern University of Science and Technology, School of Life Sciences Dean

2019-now Shenzhen Bay Laboratory Greater Bay Biomedical InnoCenter Senior principal investigator

2004-2020 Shenzhen PKU-HKUST Medical Center Associate Director, Institute director

1995-2020 Hong Kong University of Science and Technology Professor, senior researcher

1995-2020 State Key Laboratory of Molecular Neuroscience, Hong Kong University of Science and Technology Associate Director

Postdoctoral Fellow, Ontario Cancer Institute, University of Toronto (Canada) 1994-1995

Educational Background:

B.Sc. in Chemistry, Fudan University (Shanghai, P.R. China) 1984-1988

Ph.D. in Biochemistry, University of Calgary (Calgary, Canada) 1989-1993

Postdoctoral Fellow, Ontario Cancer Institute, University of Toronto (Canada) 1994-1995

Honors & Awards:

2002 Outstanding Overseas Young Scientist Award by the Natural Science Foundation of China

2003 The Croucher Foundation Senior Research Fellow Award

2006 The State Natural Science Award (Second Prize)

2011 The Ho Leung Ho Lee Foundation Science and Technology Advancement Award

2021 C.C. Tan Life Science Achievement Award

2, Dr. Nan Hu:

Information technology teacher at Shenzhen Middle School, Host of the Shenzhen Middle School Doctoral Studio for Science and Technology Innovation.

Education: PhD in Electronics and Computer Science from the University of Southampton, UK (sponsored by Chinese Scholarship Council)

Positions and awards:

- Overseas High-Caliber Personnel (level C) in Shenzhen
- Guangdong Excellent Innovation and Entrepreneurship Instructor Award of the 8th China International "Internet+" Innovation and Entrepreneurship Sprout Track Project
- Excellent Instructor Award for the "National Primary and Secondary School Information Technology Innovation and Practice Competition" Al Creator Competition
- Silver Award for Outstanding Supervisor in GBASPC Greater Bay Area Science Project Competition
- Excellent Supervisor for High School Student Newspaper